

ResearchOnline@JCU

This is the

Accepted Version

of a paper published in the journal: Continental Shelf
Research

Petus CC, Marieu V, Novoa S, Chust G, Bruneau N and
Froidefond JM (2014) *Monitoring spatio-temporal
variability of the Adour River turbid plume (Bay of Biscay,
France) with MODIS 250-m imagery*. Continental Shelf
Research, 74. pp. 35 – 49

<http://dx.doi.org/10.1016/j.csr.2013.11.011>

Monitoring spatio-temporal variability of the Adour River turbid plume (Bay of Biscay, France) with MODIS 250-m imagery.

Caroline Petus^{a, b}, Vincent Marieu^a, Stefani Novoa^d, Guillem Chust^d, Nicolas Bruneau^c and Jean-Marie Froidefond^a.*

^a University of Bordeaux, UMR EPOC 5805 CNRS, Avenue des Facultes, 33405 Talence Cedex, France.

^b Centre for Tropical Water & Aquatic Ecosystem Research (TropWATER), Catchment to Reef Research Group, James Cook University, Townsville, QLD 4811, Australia (Present address).

^c British Antarctic Survey, High Cross, Madingley Road, CB30ET Cambridge, UK

^d AZTI—Tecnalia, Marine Research Division, Herrera Kaia Portualdea z/g, 20110 Pasaia, Spain.

* Corresponding author: Tel: +33 5 40 00 88 31 ; Fax: + 33 5 56 84 08 48

Abstract

Increased loads of land-based pollutants through river plumes are a major threat to the coastal water quality, ecosystems and sanitary health. Identifying the coastal areas impacted by potentially polluted freshwaters is necessary to inform management policies and prevent degradation of the coastal environment. This study presents the first monitoring of the Adour River turbid plume (south-eastern Bay of Biscay, France) using multi-annual MODIS data. Satellite data are processed using a regional algorithm that allows quantifying and mapping suspended matter in coastal waters. The results are used to investigate the spatial and temporal variability of the Adour River turbid plume and to identify the risk of exposure of coastal ecosystems to the turbid plume waters. Changes in river plume orientation and spatial extent as well as suspended matter discharged through the river are correlated to the main hydro-climatic forcings acting in the south-eastern Bay of Biscay. The Adour River turbid plume is shown to be a highly reactive system mainly controlled by the river discharge rates and modulated by the wind changes. Despite the relatively small size of the Adour River, the Adour River turbid plume can have a non-negligible impact on the water quality of the southern Bay of Biscay and the MSM and associated contaminants/nutrients transported within the Adour turbid river plume have the potential to be disseminated far away along the northern shoreline or offshore. The main areas of influence of the river plume are defined over multi-annual (3 years) and seasonal periods. The results presented in this study show the potential of 250-m MODIS images to monitor small river plumes systems and support management and assessment of the water quality in the south-eastern Bay of Biscay.

Key words: water quality, River plume, MODIS-Aqua; mineral suspended matters, spatio-temporal variability, Adour estuary.

1. Introduction

Assessment of water quality has become a major issue worldwide and is illustrated in Europe by the implementation of the Water Framework, the Quality of Bathing Waters and the Marine Strategy Framework Directives in 2000 (WFD, 2000/60/EC), 2006 (QBWD, 2006/7/EC) and 2008 (MSFD, 2008/56/EC), respectively. These directives mainly focus on preventing the degradation of aquatic ecosystems due to anthropogenic pressures. The evaluation of the water quality status is based on the measurement of relevant water quality parameters. Among biological parameters are the composition, abundance and biomass of phytoplankton, the frequency and intensity of blooms and their influences on the water turbidity (Borja et al. 2011, Ferreira et al., 2011). Physico-chemical elements include water transparency, thermal conditions, salinity, nutrient and specific pollutants concentrations; and the influence of freshwater flows and the direction of prevailing currents are considered among hydro-morphological elements (Devlin et al., 2007). Bacterial concentrations of intestinal enterococci and *Escherichia coli* are considered into the QBWD Directive (Bergeron, 2007).

River plumes are the major transport mechanism for nutrients, sediments and other land-based pollutants into the coastal waters (e.g. Dagg et al., 2004) and play a fundamental role in the biological, geochemical and physical functioning of the sensitive coastal environment. Particulate matter discharged through the river plumes can be associated with metallic pollutants, coming mainly from industrial discharges in the watersheds, as well as with bacteria affecting coastal water quality and human health. Studies have shown that *E. coli* and enterococci bacteria are often associated with sediment discharged by rivers and that their concentrations increase in the estuaries and river plumes during storms and flood events (Bergeron, 2007; Jeng et al., 2005). By draining nutrients from domestic, industrial and agricultural effluent, fluvial discharges modify the concentrations, ratios and vertical fluxes of nutrients in the coastal domains. Nutrients play a direct function in the phytoplankton development and higher trophic levels growth. Nutrient over-enrichment can cause degradation of water clarity by supporting blooms of micro- and macro-algae and promote eutrophication (e.g. Brodie et al., 2010, Devlin and Brodie, 2005; Edmond et al., 1981). River plumes can influence the temperature and salinity of adjacent waters and also modulate strong convergence, vertical velocities and mixing in the frontal region (e.g. Orton et al., 2005). Coastal river plumes are the main pathways from the continent to the ocean. They have impacts on the majority of environmental parameters identified in the European Directives. It is thus particularly important to monitor the coastal river plumes and understand the processes controlling their spatial and temporal variability to prevent degradation of the water quality and coastal ecosystems. This includes determining their area of influence along coastlines, their sedimentary variability, and how these parameters evolve in response to internal and external forcings.

Rivers plumes are subjected to the Coriolis Effect and, in the northern hemisphere, are theoretically deflected to the right when they flow from estuary mouths. In the absence of strong external hydro-climatological forcing, a northern hemisphere river plume will turn anticyclonically and attach to the coast, where it then merges into a coastal current (Geyer et al., 2004; Wiseman and Garvine, 1995). However, spatial and temporal variations in river plume events are modulated by a number of factors including storms and discharge strength (e.g. Lahet and Stramski, 2010, Lihan et al., 2008), coefficients and tidal cycles (e.g. Valente and da Silva, 2006), magnitude and direction of wind stress (e.g. Dzwonkowski and Yan, 2005; Lentz and Largier, 2006; Lihan et al., 2008) or bathymetry and exit angle (e.g. Lee and Valle-Levinson, 2012). This variability makes traditional measurement methods

such as shipboard surveys or mooring arrays insufficient. Many studies have shown that remote sensing methods such as video camera, airborne or satellite imageries are efficient complementary tools for river plume monitoring because of their adapted spatial and temporal resolutions (e.g. Dailloux, 2008; Doxaran et al., 2009; Lihan et al., 2008; Morichon et al., 2008; Nezlin et al., 2007; Thomas and Weatherbee, 2006; Warrick et al., 2007). More particularly, satellite images provide synoptic and frequent regional overviews that enable more effective analysis of the river plume spatial and temporal distribution, using optically active parameters that can be measured from space by the ocean colour (Lihan et al., 2008). Suspended matter increase the backscatter in large wavelengths of the visible spectrum while the CDOM and chlorophyll-a (Chl-a) absorb light in the lower wavelengths (Froidefond and Doxaran, 2004). The optical river plume signature is thus related to the presence and combination of these parameters in the water.

This study focuses on a turbid river plume discharged through the Adour River, a relatively small river (309 km) located in the south-eastern Bay of Biscay (France). The Adour estuary drains a highly anthropogenised catchment area, host the 9th national commercial port in France and local beaches surrounding the estuary constitute a major touristic area; including intense recreational coastal activities (Arleny et al., 2007) that peak during the summer-early autumn season. The estuary also supports an important biodiversity including the endangered *A. Anguilla* species, which absorbs heavy metals and organic pollutants (e.g. Arleny et al., 2007; Tabouret et al., 2011). The estimated suspended solids flow entering into the estuary is about 0.25 Mt.yr^{-1} (Etcheber et al., 2007; Maneux et al., 1999). Previous studies of Bergeron (2007) and Bareille et al. (2006) confirmed the role of the Adour River turbid plume as a means of transport of faecal pollutions, particularly during high river outflows when germs coming from the watershed are transferred to the littoral waters. Furthermore, as metallic pollutants are often associated to sediments (Stoichev et al., 2004), the Adour estuary may represent a non-negligible contribution of contaminant input into the Bay of Biscay. Because of the great economical, touristic and ecological significance of the Adour estuary and its surrounding coastal waters, there is an increasing interest on the environmental impact of the Adour River turbid plume (Bergeron, 2007; Dailloux, 2008; Ferrer et al., 2009; Jegou et al., 2001; Morichon et al., 2008; Novoa et al. 2012a,b,c; Sagarminaga et al., 2005). However, the local scientific knowledge is still poorly developed in comparison to other French or international river plumes, such as the Gironde River plume or the Great Barrier Reef river plume system for example, where there exists a more substantial information base to support management and assessment of the water quality (e.g. Artigas, 1998; Devlin et al., 2012, Froidefond et al., 1991; 1998; Labry et al., 2005; Lazure and Jegou, 1998; Schroeder et al., 2012).

An empirical regional algorithm has been developed by Petus (2009) and Petus et al. (2010) to map the total suspended matter (TSM, in mg.l^{-1}) concentrations within the Adour River turbid plume using Moderate Resolution Imaging Spectroradiometer (MODIS) 250-m imagery. In the present study, 246 daily MODIS scenes selected between years 2006 and 2009 are processed by this algorithm. The main objective of this study is to monitor the seasonal and inter-annual spatio-temporal variability of the Adour River turbid plume across the south-eastern Bay of Biscay. Specific objectives are to develop an automated supervised method to map and delineate the river plume area, to assess the ranges of sediment concentration discharged through the river plume, to define the spatial risk of exposure from river plume waters to inshore marine waters and to relate information on spatial and temporal variability of river plumes derived from satellite images to the main hydro-climatic forcings acting in the southern Bay of Biscay.

2. Study area

2.1. Adour estuary and coastal waters

The study area is located on the south-eastern part of the Bay of Biscay (Figure 1a), where coastal ecosystems receive continental waters from the turbid outflow plume of the Adour River (Figure 1b and c). The Adour estuary is a meso- to macro-tidal system characterised by a tidal range between 2 and 5 m (Stoichev et al., 2004) and energetic wave conditions (Abadie et al., 2005). The mean annual river discharge is about $300 \text{ m}^3 \cdot \text{s}^{-1}$ and reaches $2000 \text{ m}^3 \cdot \text{s}^{-1}$ during brief flood events (Stoichev et al., 2004). The Adour watershed, covering about 17000 km^2 , connects the occidental Pyrenean piedmont to the Atlantic Ocean. The drainage basin is composed of the Adour, Bidouze, Gaves, Nive, Luy and Nivelle hydrographical contributor basins.



Figure 1: a) Study area in the South West of France. The Adour turbid plume viewed from b) a field picture (6th of June, 2007) and c) MODIS-Aqua 1-km imagery (colour composite, 16th of March, 2006). The Adour estuary forms the boundary between the northern Landes littoral (L) and the Southern Basque Littoral (B).

The geomorphological characteristics of the estuary, the hydrological features and the channelled waterways of the estuarine section lead to short residence time for both water and particles, ranging from a few hours to several days (Point et al., 2007; Villate et al., 1989). Therefore, sedimentation rates are low in the estuary and most of sediment inputs from the river are rapidly exported to the ocean (Maneux et al., 1999). Point et al. (2007) estimated that 75% of the annual flux of suspended solids of the Adour River is exported to the ocean within 30-40 days and the solid discharge of the Adour River has been calculated about $0.25 \text{ Mt} \cdot \text{yr}^{-1}$ (Maneux, 1998).

The upstream part of the estuary flows through agricultural areas, while the downstream part is within the urban district of Bayonne and is subject to industrial inputs (Stoichev et al., 2004). The estuary collects waters from a population about one million inhabitants, mainly located in medium cities along the river continuum (Monperrus et al., 2005). The Adour estuary forms the boundary

between the northern Landes littoral and the southern Basque littoral (Figure 1c). The Basque and Landes countries welcome a high number of tourists, particularly on the coastal area during the summer period. The Adour estuary is thus under a strong anthropogenic pressure due to urban, agricultural and industrial activities (Arleny et al., 2007; Brunet and Astin, 1999).

2.2. The Adour River turbid plume spatio-temporal variability

Three studies recently investigated the Adour River turbid plume spatio-temporal variability using respectively: a 5-km grid hydrodynamic model simulating the sea surface salinity during the year 1995 (Jegou et al., 2001), forty-four 8-days 250-m resolution MODIS surface reflectance composites covering the year 2004 (Sagarminaga et al., 2005) and a selection of 0.1 to 100-m resolution video images during the year 2008 (Dailloux, 2008; Morichon et al., 2008). The different temporal and spatial resolutions of these complementary studies provided the first insights into the Adour River turbid plume spatio-temporal variability. The main area of influence of the Adour River turbid plume was estimated about 8.4 km², with a south-western orientation modulated by the hydrologic and climatic forcings (Sagarminaga et al., 2005). Statistical relationships (determination coefficient $R^2 = 0.8$) were obtained between the Adour river discharge rates and the river plume areas detected by the shore-based video system (Dailloux, 2008). However, the cameras layout and view angle (restricted to the estuary mouth) prevented to monitor river plume surfaces larger than 0.045 km². Past studies also showed that wind can modify the river plume width and orientation, with strong northern winds potentially reversing the Coriolis-driven plume direction (Dailloux, 2008; Jegou et al., 2001). Finally, under low river outflow or high flood tidal velocity conditions, pulsed river discharged river plumes modulated at the tidal frequency were observed by Dailloux (2008). Nevertheless, these studies only gave sporadic assessment of the Adour plume spatio-temporal variability.

3. Material and methods

3.1. MODIS-Aqua 250-m imagery

Long-term, medium resolution, optical satellite imagery provides a good understanding of coastal water quality fluctuations over the time and a strong baseline for assessment of changes. This study is based on MODIS-Aqua surface reflectance data (MYD09). This data are freely available since 2002 with a spatial resolution of 250 m, at high frequency (1/day), and allow the monitoring of the Adour River turbid plume over a multi-annual time period.

MODIS-Aqua surface reflectance data are geolocated and are provided by the NASA (<http://reverb.echo.nasa.gov/reverb/>) in a Sinusoidal Grid (SIN) projection with standard tiles representing 10 degrees by 10 degrees. MODIS L1B data (calibrated and geolocated radiances), used as primary input, are corrected for the effect of gaseous absorption, molecules and aerosol scattering, coupling between atmospheric and surface bi-directional reflectance function and adjacency effect (Vermote et al., 1997). Gaseous absorption and molecular scattering are computed based on the viewing and solar angles and using look-up tables. The aerosol scattering is computed using dark targets for which empirical relationships have been established between the visible and short wave infrared reflectance (Kaufman et al. 1997). The result is an estimate of the seawater reflectance (R) which is not accurate enough for open ocean applications. However Doxaran et al.

(2009) demonstrated that this product can be appropriate for monitoring reflective turbid waters, as the Adour River turbid plume. This product is easy to process (see explanations in Doxaran et al., 2009) and, for a practical and operational point of view, was considered in this study.

We used the MODIS bands 1 'surface reflectance' product centred at 645 nm (R645) as a proxy for the turbidity (sediment-dominated) levels. A regional empirical algorithm (Equation 1) was developed (Petus, 2009; Petus et al., 2010) to monitor the TSM concentration using MODIS bands 1 'surface reflectance' product centred at 645 nm.

$$\text{TSM} = 12450x^2 + 666.1x + 0.48 \quad \text{Equation 1}$$

where x is the remote sensing reflectance measured by the MODIS band 1 ($R_{rs}(B1)$) and $R_{rs}(645) = R(645)/\rho_i$.

The regional algorithm used to calibrate the MYD09 band 1 (Equation 1) was developed from in-situ measurements collected in the Adour River turbid plume (Petus, 2009; Petus et al., 2010). This polynomial algorithm was successfully applied to MODIS bands 1 surface reflectance data centred at 645 nm to map TSM concentrations within the Adour River turbid plume for a collection of date between 2006 and 2009 (Petus, 2009; Petus et al., 2010). These maps were further validated through comparison with mineral suspended maps produced applying IFREMER empirical algorithms (e.g. Gohin et al., 2002; 2005) to MODIS 1000-m resolution imagery processed with Seadas (Baith et al., 2001). Despite their different processing and atmospheric correction procedures, maps at 250-m and 1000-m resolutions showed good consistency, except for suspended matters concentrations higher than 30 mg l^{-1} (Petus et al., 2010).

3.2. Calibrated map database

For this study, 246 MYD09 cloud-free scenes on our study area were selected between January 2006 and April 2009 (MODIS DataBase: MDB). The selection of days without cloud coverage or with minimal cloud impact over the Adour River turbid plume area was visually made using the "NAvigating throUgh Satellite and In situ data over loCAL Areas (NAUSICAA, Gohin et al., 2002; Gohin et al., 2005) internet platform displaying MODIS images on our study area. A mask based on the reflectance measured in the MODIS band 2 (859 nm) was applied to remove most of the cloud contamination (Doxaran et al., 2009; Petus, 2009). A Matlab routine was developed to reproject the raw MYD09 data using the MODIS Reprojection Tool (MRT, Dwyer and Schmidt, 2006) and to select and map the total suspended matters in our study area [1.3°O , 43.2°N ; 1.9°O , 43.9°N] using the TSM regional algorithm (Equation 1, Petus, 2009; Petus et al., 2010).

In the Adour turbid coastal waters, mineral suspended matters represent the major proportion of the total suspended matters in terms of weight, while the contributions of planktonic and detrital organic particles are low or even negligible (Petus, 2009; Petus et al., 2010). Therefore, we considered the synoptic maps of total suspended matters (TSM, mg.l^{-1}) obtained to be representative of the mineral suspended matters concentrations (MSM, mg.l^{-1}) in water.

3.3. Data analyses procedure

The Adour River turbid plume influence is easily identifiable on the 250-m MSM maps and is illustrated by high mineral suspended matter concentrations close to the estuary mouth and decreasing concentrations with the distance from the coast (Figure 2, step 1). In order to study the river plume spatio-temporal variability, data were analysed in four steps: (1) maps of the Adour River turbid plume were produced; (2) indices characterising the temporal hydro-sedimentary variability of the river plume were computed, (3) the spatial impact area of the river plume was estimated and, (4) information obtained on the spatial and temporal variability of Adour River turbid plumes was related to the main hydro-climatic forces acting in the south-eastern Bay of Biscay.

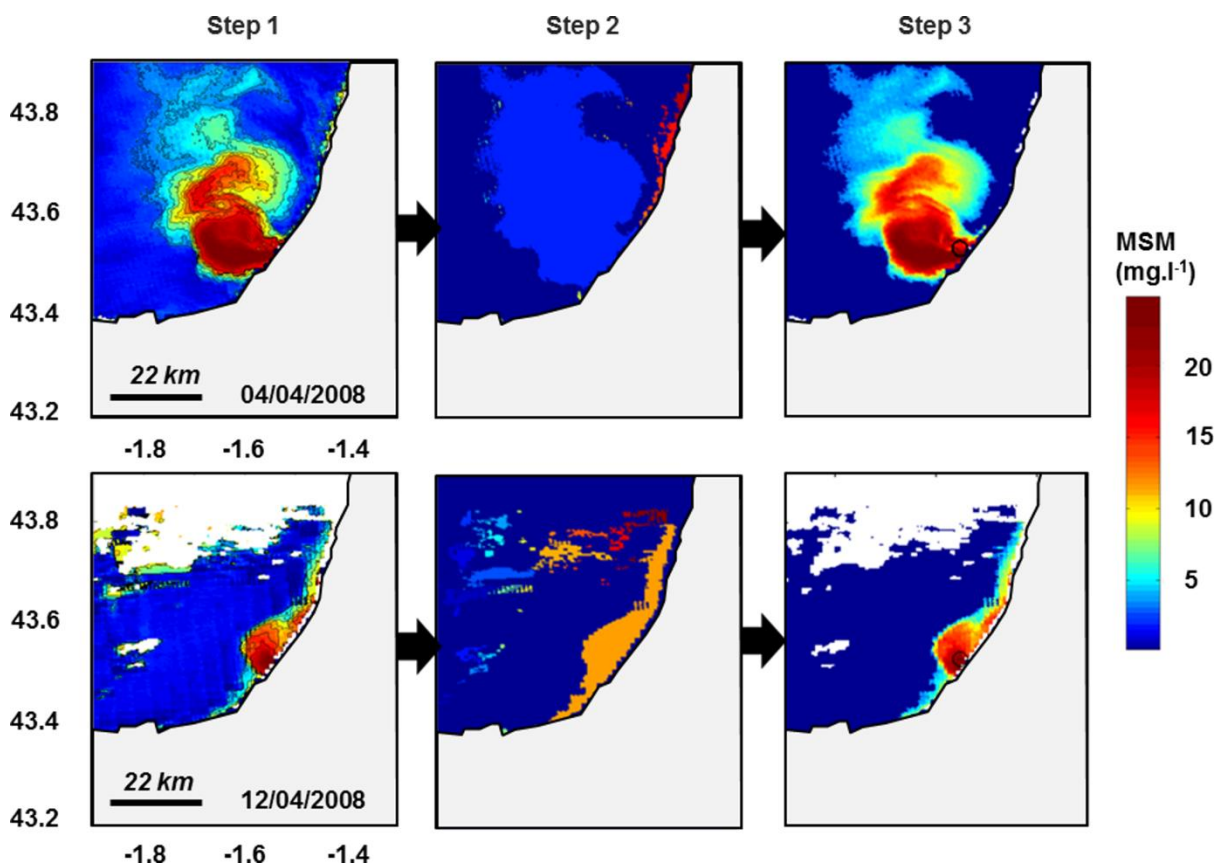


Figure 2: Supervised detection of the Adour plume by a fixed Mineral Suspended Matter concentration threshold of 3 mg.l^{-1} . Step 1: display of the MSM iso-concentration lines on the MODIS maps; step 2: identification of MSM areas $> 3 \text{ mg.l}^{-1}$; step 3: selection and re-map of the closest area to the mouth, identified as the plume area. The location of the Adour estuary is indicated with black circles.

In order to delineate the Adour River turbid plume (rich in mineral suspended matters) from the surrounding coastal waters (clearest waters), a threshold approach was adopted. A threshold of 3 mg.l^{-1} was established above which MSM values were considered to be indicative of the Adour River turbid plume presence. This threshold was defined based on the study of Petus et al. (2010) describing seawaters subject to direct inputs of Adour runoff with salinity ranging from 17 to 28 PSU, temperature between 18 and $22 \text{ }^\circ\text{C}$ and TSM concentrations between 3 and 16 mg.l^{-1} . The threshold

of 3 mg/l coincides also with a gradient in salinity as shown by Figure A in appendix. A Matlab routine was developed to apply this threshold delineation and to map the river plume area from each of the 256 daily MSM maps (Figure 2). First, the concentration contours (or iso-concentration lines, in mg.l^{-1}) are calculated and drawn on the 250-m MSM maps (Figure 2, step 1). Subsequently, the areas with $\text{MSM} > 3 \text{ mg.l}^{-1}$ are identified (Figure 2, step 2). These areas correspond both to the Adour River turbid plume and to the nearshore areas where wave induced resuspension of sediments (red areas on Figure 2, step 2, 04/04/2008) or unmasked cloudy pixels (northern areas on Figure 2, step 2, 12/04/2008). In order to restrict the analyses to the Adour River turbid plume area and limit the influence of sediment resuspension processes close to the coast, only the continuous area nearest to the Adour estuary mouth is selected (Figure 2, step 3). River plume area maps are then created by masking all pixels located outside this selected area. This methodology permits identification and delineation of the Adour River turbid plume and also allows for the removal of highly reflective pixels contaminated by sediment resuspension or cloud cover, except for the corresponding pixels connected to the Adour area.

In order to study surface area changes of the Adour River turbid plume, the number of pixels within the river plume boundary was computed and converted to area (in km^2) of river plume for each of the daily MODIS-MSM images. The daily maximal and average MSM daily concentrations (C_{max} and C_{mean} , respectively, in mg.l^{-1}) were also calculated within the delimited Adour River turbid plume to document ranges of sediment concentration discharged through the plume. Spatial analyses included the production of mean and frequency occurrence maps computed from the daily river plume areas maps. Frequency of occurrence maps were created by determining, for each pixel of our study area, the percentage of time when pixels are designated as river plume (*i.e.*, when $\text{MSM} > 3 \text{ mg.l}^{-1}$ and belong to the continuous area closest to the Adour estuary mouth). Mean maps were obtained by averaging the river plume maps and both occurrence and mean maps were calculated over seasonal, multi-annual and case-specific periods.

Finally, relationships between hydro-climatic forces and the Adour River turbid plume spatio-temporal variability were investigated. The indices chosen are (i) the Adour discharge rates at the Adour river mouth ($\text{m}^3.\text{s}^{-1}$), obtained from the Regional Environment Directories (DIREN) website (<http://www.hydro.eaufrance.fr>). Fifty-two years of daily measurements covering the 1957- 2009 period were downloaded in order to cover our study time period, and also to assess the long-term variability of the Adour River discharge. (ii) The wind intensity (m.s^{-1}) and direction ($^\circ$) measured by the NASA Quick Scatterometer (QuikSCAT) at the grid point 1,75°O, 43,75 N. Ten years of daily Level 2B QuikSCAT winds covering the 1999-2009 period were obtained from the Center for Satellite Exploitation and Research (CERSAT) extraction service (<http://www.ifremer.fr/cersat> (CERSAT-IFREMER, 2002)). (iii) The tidal coefficient (index of tidal range: small coefficients for Neap tides and large coefficients for Spring tides) and the tidal height (m) measured at the Boucau-Bayonne Port. Data covering the 2006-2009 period were obtained from the Naval Hydrographic and Oceanographic Service (SHOM) website (www.shom.fr/).

4. Results

4.1. Representativeness of the MODIS database climatic conditions

Cloud coverage over our study area prevents to work with a continuous, daily MODIS dataset. For this study, 246 MYD09 cloud-free scenes were selected between January 2006 and April 2009. This data are well distributed with 72 scenes in 2006, 77 in 2007, 75 in 2008, and 22 for 2009 first trimester.

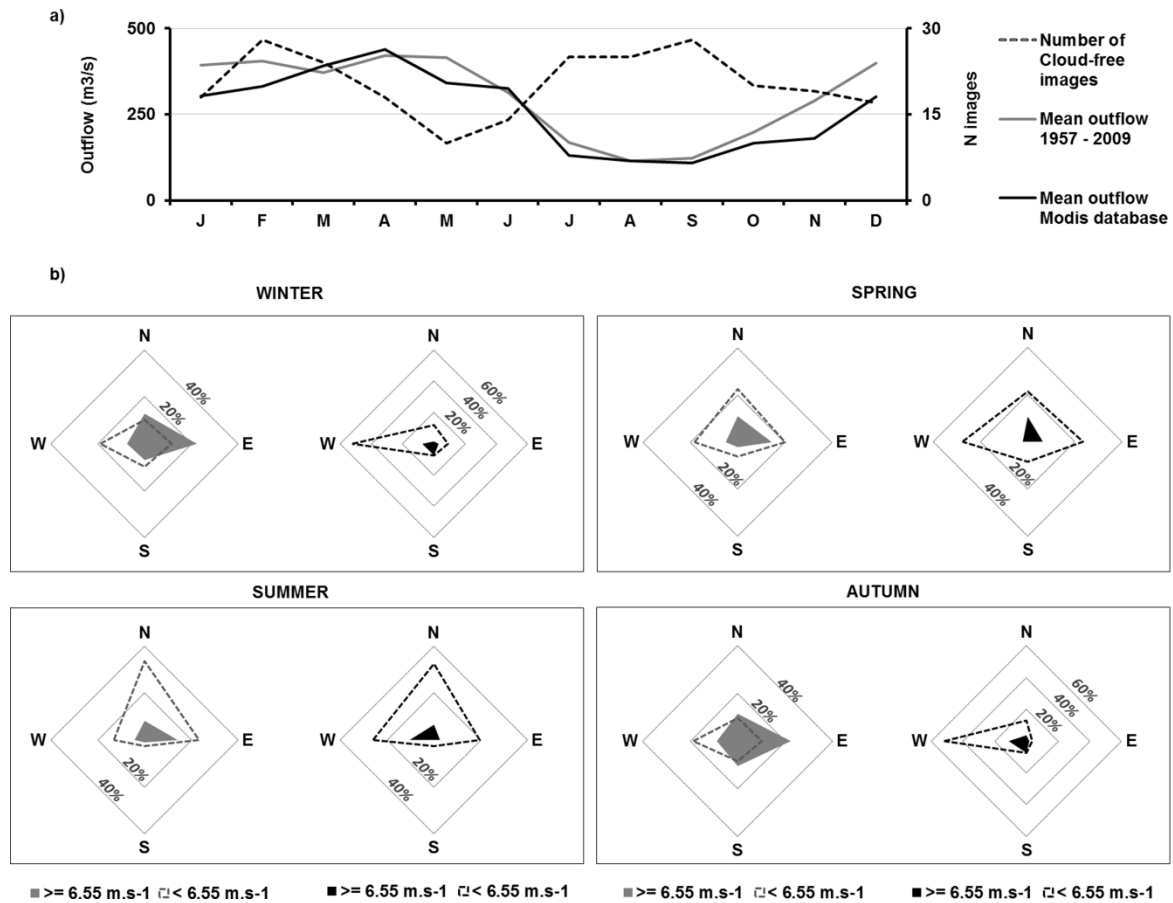


Figure 3: Representiveness of the Modis database (MDB) climatic conditions (black symbols) compared with the typical Adour climatic conditions (grey symbols) (a) mean monthly Adour River outflows calculated from 52 years of daily measurements (m³.s⁻¹, 1957-2009 period) and from the MDB flow conditions. The number of cloud free MODIS images per month is indicated with a black dashed line (N images). (b) Seasonal wind occurrence percentage calculated from 10 years of daily measurements and from the MDB wind conditions (QuikScat data). Plain surfaces and dashed lines represent the winds above and under the mean annual wind speed (6.55 m.s⁻¹), respectively; N (north), E (East), S (south), W (west) symbols are the wind directions.

As the dataset is non-continuous, we tested its representiveness by comparing the mean monthly river discharge conditions corresponding to the daily MODIS database (MDB) satellite images with the mean monthly discharge calculated from 52 years of daily discharge measurements (1957-2009 period). The analysis (Figure 3a) shows that both time series follow similar trends (Figure 3a), although underestimations in the MODIS data set of January, November and December mean discharges (mean error: 23, 38, and 24%, respectively). In both databases, maximal discharge rates

are recorded during the spring season, whilst dryer conditions are observed over the summer period. The number of satellite images available per month in the MODIS Database is inversely related to the river discharge values (Figure 3a).

Similarly, the seasonal wind occurrence percentages calculated from 10 years of daily QuickSCAT measurements and from the MDB QuickSCAT wind conditions are similar (Figure 3b). An underrepresentation of strong winds ($> 6.55 \text{ m.s}^{-1}$) is nevertheless clearly detected in the MODIS database, in all seasons. Winter and autumn regular winds ($< 6.55 \text{ m.s}^{-1}$) are mainly from West, whereas wind conditions over the summer and spring period are more variable (Figure 3b). Southerlies winds conditions are rarely recorded.

4.2. Pluri-annual spatio-temporal variability and area of influence of the Adour River turbid plume

The Adour River turbid plume is a highly dynamic oceanographic structure (Figure 4). River plume surface areas recorded in our data base range between 0.2 km^2 and 1400 km^2 , with 13% of the measured areas ranging between 0.2 and 1 km^2 , 17% from 1 to 10 km^2 , 24% from 10 to 100 km^2 and 27% from 100 to 1500 km^2 . The maximal and mean MSM concentrations recorded inside the river plume range from 3 to 71 mg.l^{-1} and 3 to 20 mg.l^{-1} , respectively. Fifty percentage of the maximum concentration (C_{max}) recorded are lower than 10 mg.l^{-1} and 70% of the mean concentration (C_{mean}) range between 3 and 5 mg.l^{-1} .

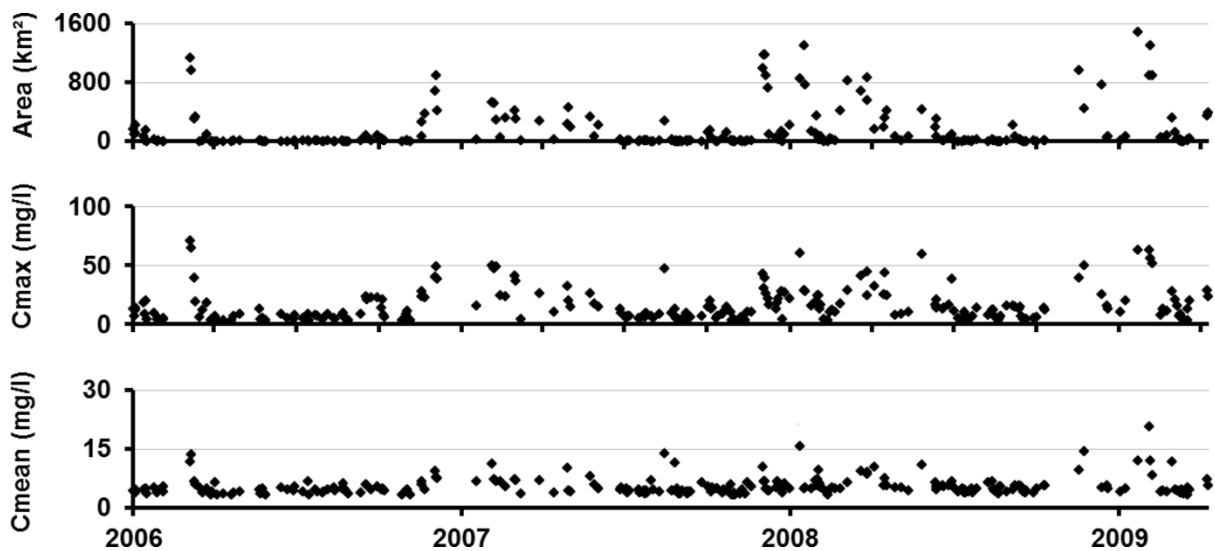


Figure 4: Multiannual plume areas (km^2) and maximal and average sediment concentration (mg.l^{-1}) recorded from the MODIS MSM maps.

Figure 5 presents a selection of large Adour River turbid plume mapped (surface area $> 200 \text{ km}^2$). They are characterized by a wide range of shapes and MSM concentrations, illustrating the high spatial, temporal and sedimentary variability of the Adour River turbid plume. In first approximation, most of these broad river plumes seem to move northward under the Coriolis effect. Comparisons between river plume areas and mean and maximum MSM concentrations, respectively, indicate

positive relationships between the size and the MSM concentration recorded inside the Adour River turbid plume (Figure 6, correlation coefficients $r = 0.81$ and $r = 0.62$, respectively).

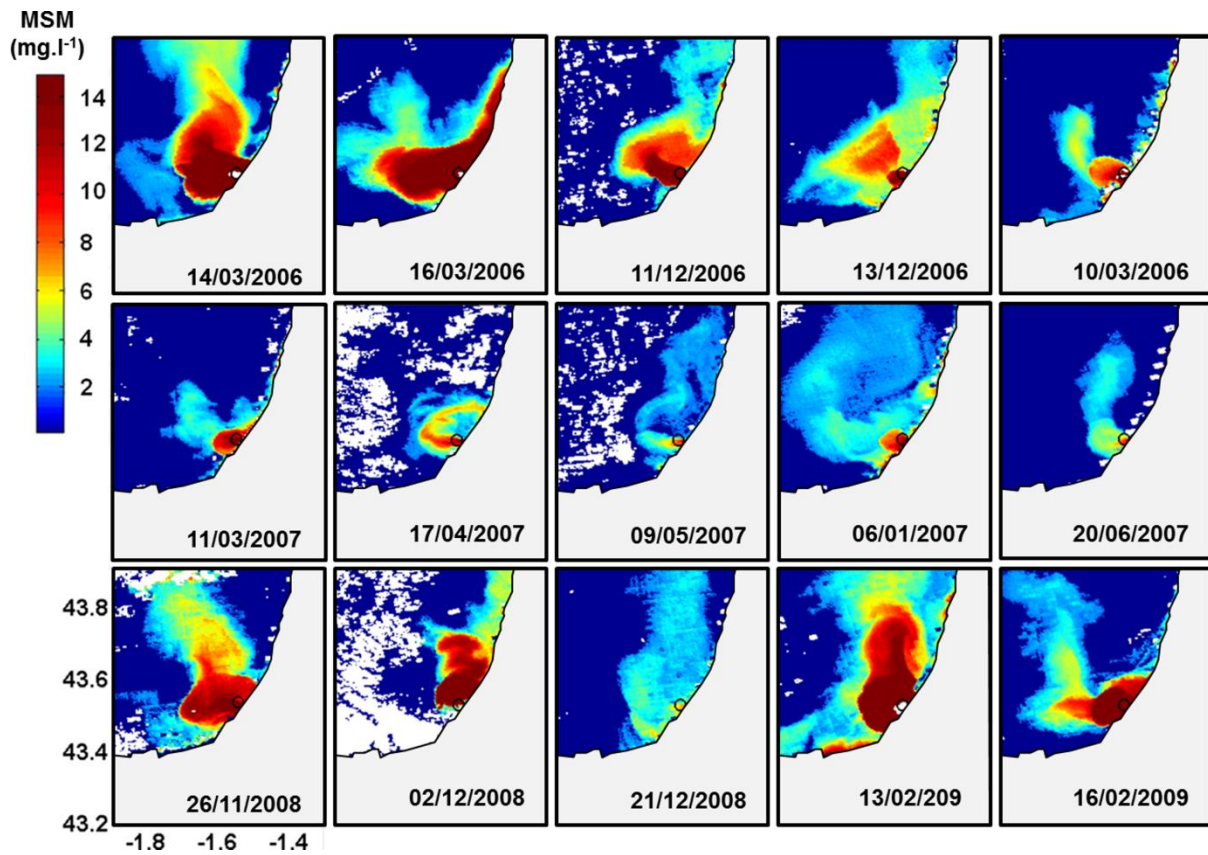


Figure 5: examples of large mapped plume (area $>200 \text{ km}^2$) illustrating the high sedimentary and spatio-temporal variability of the Adour plume.

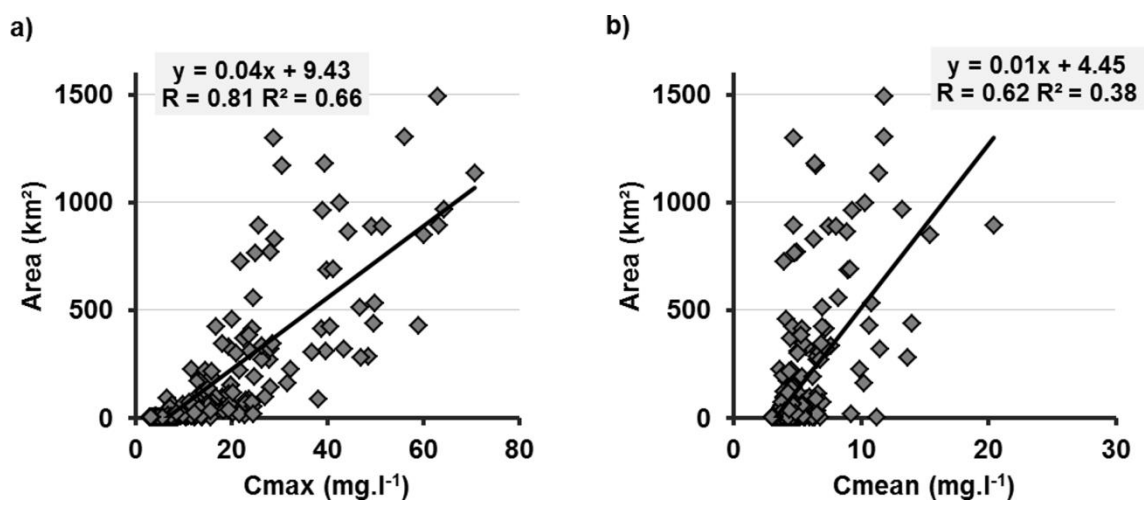


Figure 6: correlations between a) maximal (C_{max}) and b) mean (C_{mean}) concentrations recorded inside plumes, respectively, and the plume areas. Linear regressions and regression statistics are indicated on the figure.

The spatial risk of exposure from Adour River turbid plume waters to inshore marine waters is illustrated by the map of frequency of occurrence of “plume-classified” pixels (Figure 7a) and by the mean MSM concentrations map (Figure 7b) calculated over the 2006-2009 period from the 246 daily river plume area maps. In our MODIS satellite database, the Adour River turbid plume is recorded more than 60% of the time at the estuary mouth and 20% of the time as far as 10 km offshore from the estuary (-1.65°, Figure 7a).

High MSM concentrations above 3mg.l^{-1} are observed from the estuary mouth to 20 km north and 10 km south, 20% of the time (Figure 7a). However, the coastal waters closest to the southern boundary of the estuary mouth (up to the latitude of Biarritz) experience high risk of river plume exposure, with occurrence percentage ranging between 40% and 60% (Figure 7a). The same tendencies are recorded on the mean MSM concentrations map (Figure 7b), with maximal concentrations ($> 4\text{mg.l}^{-1}$) recorded from the estuary mouth to the inshore waters of Biarritz.

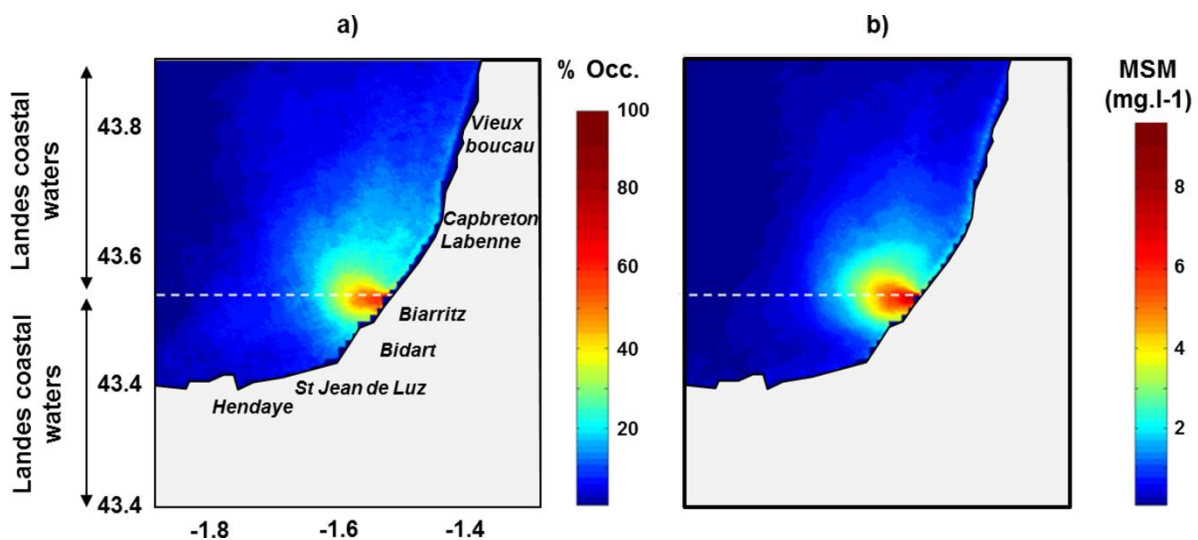


Figure 7: Geographical area of influence of the Adour plume calculated from the 246 MODIS images selected. a) Occurrence percentages (% Occ.) of MSM $> 3\text{ mg.l}^{-1}$, b) mean MSM concentrations. The Adour estuary longitude is indicated with dashed white lines. This figures map the risk of exposure to coastal ecosystems from enhanced concentrations found in Adour plume waters.

4.3. Relation to hydro-climatic forcings

4.3.1. Discharge rates

River discharges are positively correlated with Adour River turbid plume areas and MSM concentrations detected by satellite (Figure 8a). Discharge rates at the river mouth measured on the day of satellite acquisition explain 46%, 57% and 54% of the surface area, C_{max} and C_{mean} index variances, respectively (Figure 8a). Lower determination coefficients ($R^2 < 0.3$) are obtained using 1 to 3 days lag discharges data. Statistical analyses of our area index show that discharges over $400\text{ m}^3.\text{s}^{-1}$ systematically lead to a river plume area larger than 10 km^2 and river plume areas larger than 50 km^2 are not recorded for river discharges lower than $100\text{ m}^3.\text{s}^{-1}$.

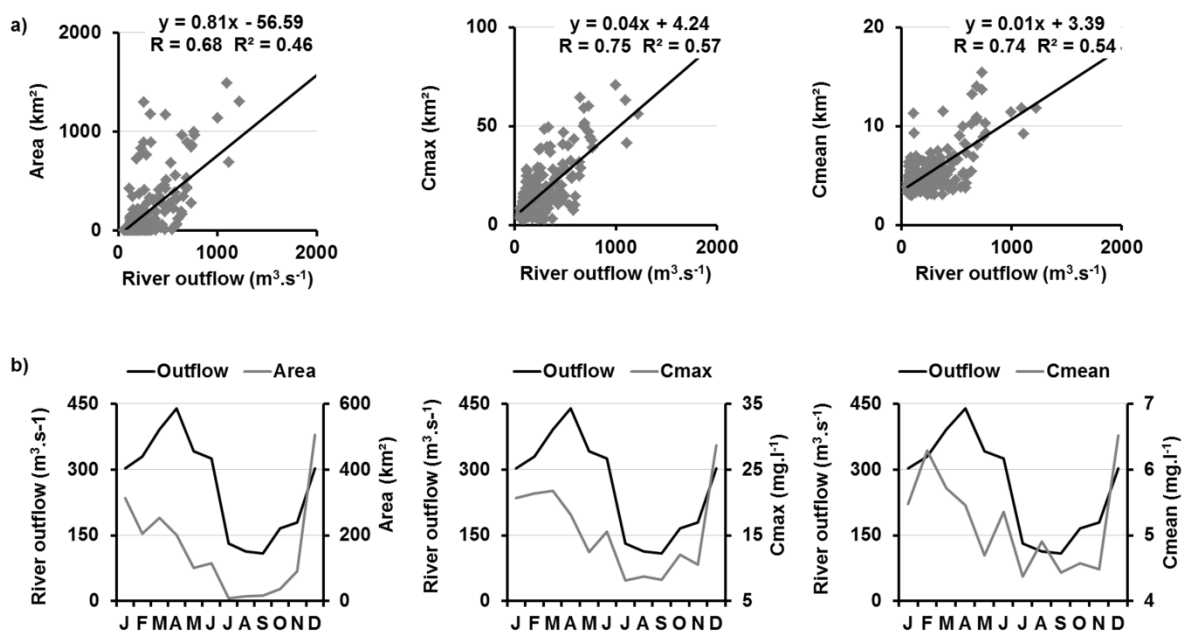


Figure 8: (a) correlations between daily MDB river outflows and (respectively from left to right) areas, maximal concentrations and mean MSM concentrations recorded inside plumes during the 2006-2009 period. Linear regressions and determination coefficients calculated are indicated. (b) Mean monthly plume area, Cmax and Cmean (black lines) and MDB Adour river outflows (grey lines).

Similar trends between river discharges and the Adour River plume surface areas and MSM concentrations are also observed at the seasonal scale (Figure 8b). The mean monthly river plume surface areas decrease from January to May months (mean value of 313 to 101 km²) and are minimum (<20 km²) between July to September months. A slight increase of the river plume surface area is nevertheless observed during June (115 km²). River plume spread out again from October and a maximal river plume area is recorded during December (506 km²). The mean monthly maximal concentrations follows the same trends with maximal MSM concentrations recorded from December to April months (mean value of 29 to 18 mg.l⁻¹), low concentrations during the summer period (Cmax < 10 mg.l⁻¹) and slightly higher MSM values measured during the June month (Cmax = 16 mg.l⁻¹). The averaged MSM concentrations are more relatively more constant all around the year (from 4 mg.l⁻¹ during the summer period to 7 mg.l⁻¹ during the December month), although following similar trends.

4.3.2. Wind conditions

Figure 9 presents the Frequency of occurrence maps of MSM > 3 mg.l⁻¹, and the mean MSM concentration maps calculated from MODIS images grouped in function of the main wind direction measured on the day of satellite acquisition. Eastern winds promote the Adour River turbid plume expansion westward (offshore) and northward of the estuary mouth (Figure 9a). However, under eastern to south-eastern wind conditions the Adour River turbid plume orientation is less obvious and the Adour River turbid plume expands 20 % of the time towards the south-west. Under southern

winds the river plume expands towards the North and this wind orientation promotes the river plume attachment to the coast (Figure 9b). Further north, high MSM concentrations are observed 20 % of the time in a coastal band which expands beyond our maps boundaries. Western winds also tend to push the turbid freshwater toward the coast but the northern highly concentrated coastal band is no more observed (Figure 9c). Finally, northern winds expand the Adour River turbid plume toward the South-west of the estuary mouth (Figure 9d). However, a secondary plume orientation toward the North is clearly observable, particularly under N-NW wind conditions.

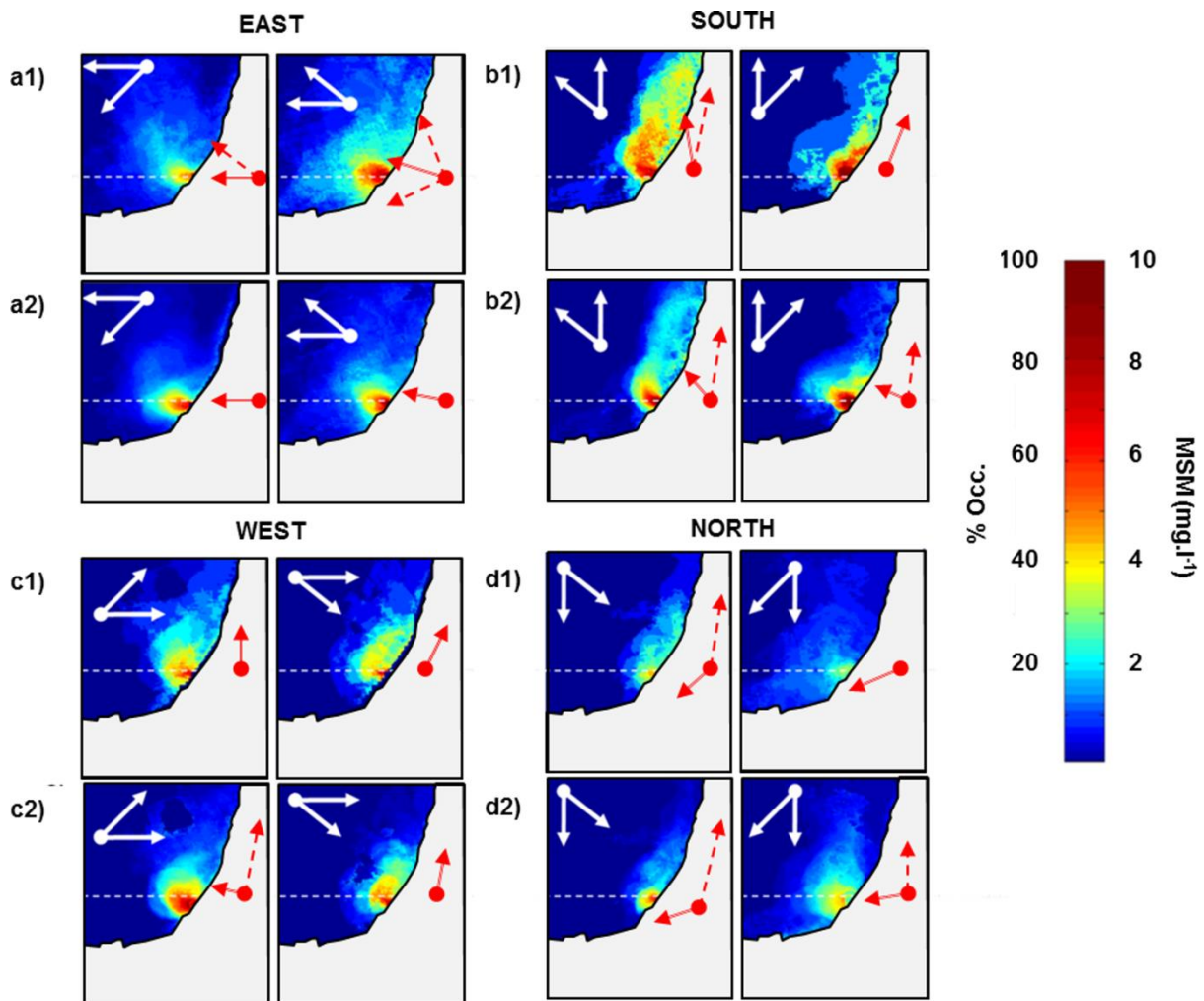


Figure 9: Influence of wind patterns on the Adour plume orientation. 1) Occurrence percentages of MSM > 3 mg.l-1 and 2) mean MSM concentrations for a) easterlies, b) southerlies, c) westerlies and d) northerlies winds. Wind orientations are indicated in white. Primary (Occ. = 40% and MSM = 4 mg.l-1) and secondary plume propagation orientations are symbolised (Occ. = 20% and Cmax = 2mg.l-1) by double and dashed red arrows respectively.

4.3.3. Tidal conditions

Tides of the southern part of France can influence the coastal processes on two temporal scales: semi-diurnal (measured by the tidal height index) and lunar (measured by the tidal coefficient index). No linear correlation could be found between the tide indices and the computed river plume surface areas and concentrations (Cmax and Cmean). However, our results suggest that tides affect the Adour River turbid plume areas and concentrations. Over the 2006-2009 period, when the tidal heights measured at the Adour estuary mouth are lower or equal to 3 m, the river plume areas are on average 90 km² larger than the river plume areas observed under higher tide (> 3 m). On the same case scenario, the Cmax and Cmean recorded inside the river plume boundaries are 7.4 and 0.7 mg.l⁻¹ higher, respectively. For the highest spring tides (tidal coefficients > 70), river plume areas are on average 90 km² larger than the river plume areas observed under lower tidal coefficient conditions (tidal coefficients ≤ 70). On the same case scenario, the Cmax and Cmean recorded on the Adour River turbid plume are 3.3 and 0.5 mg.l⁻¹ higher, respectively.

Table 1: Average Adour River turbid plume area and maximum and mean MSM concentrations measured over the 2006-2009 period and under specific tide conditions (Coef: tidal coefficient the Htide: tidal height)

Tide condition		Area (km ²)	Cmax (mg.l ⁻¹)	Cmean (mg.l ⁻¹)
Htide (m)	≤ 3	172.67	17.44	5.39
	>3	82.12	10.03	4.72
Coef.	≤ 70	121.24	3.68	4.97
	> 70	172.99	16.95	5.43

5. Discussion

5.1. Data and methodology

Satellite imagery provides the synoptic view necessary for inventory and mapping of ecological systems (Hewitt and Mason, 1990). The different spatial and temporal resolutions of sensors are complementary for conducting comprehensive environmental monitoring. Previous studies have demonstrated that remote sensing imagery can be used to study river plume spatio-temporal variability. However, most of these studies have focused on plumes discharged through relatively large river systems and were based on 1-km resolution satellite data (e.g. Dzwonkowski & Yan, 2005; Warrick et al., 2007). In this study, we used the medium resolution (250-m) MODIS bands 1 surface reflectance product. Chen et al. (2007) and Hu et al. (2004) demonstrated that the quality of the

MODIS land band 1 is adequate for producing remote sensing products of coastal waters. There is a strong correlation between the suspended sediment concentrations in turbid environments and the MODIS band 1 (e.g. Miller and McKee 2004; Doxaran et al. 2009; Petus et al. 2010; Ondrusek et al., 2012). Radiance or reflectance values measured in the band 1 have been used as qualitative proxy for amounts of total suspended matter (TSM) (e.g. Lahet and Stramski, 2010) or integrated in empirical bio-optical algorithms to quantify the concentrations of TSM (mg.l^{-1}) or the turbidity levels (NTU) in marine waters (e.g. Miller and McKee 2004, Petus et al. 2010). This study underlines how this high resolution data along with hydro-climatic data can be used to enhance our general knowledge about small river plumes systems.

We choose to work with MYD09GQ products available on the NASA website. A discussion on the practical and operational interest of using the MYD09 product is presented in Doxaran et al. (2009). Atmospheric corrections of MYD09GQ products are not accurate enough for open ocean applications although considered appropriate in the case of reflective; *i.e.*, turbid coastal environments such as the studied area (Doxaran et al., 2009, Petus et al., 2010). The results obtained extend previous sporadic studies undertaken in south Eastern Bay of Biscay (Jegou et al., 2001; Morichon et al., 2008; Sagarminaga et al., 2005) and demonstrate the potential of 250-m MODIS surface reflectance product for monitoring the Adour turbid river plumes over a multi-annual time period. Moreover, the MSM regional algorithm (equation 1) and the threshold methodology employed (Figure 2) increased the knowledge about the spatio-temporal variability of the Adour River turbid plume.

MODIS time-series used in this study are not continuous and number of cloud free images available on our study area is inversely proportional to the Adour River discharge (Fig 3a). These observations underline the climatic limitations of our satellite-based methodology. Strong Adour River discharge rates are associated with stormy or windy conditions and characterized by high rainfall conditions and cloud coverage. This cloud contamination prevents ocean colour observations and the description of the Adour River turbid plume through optical satellites images. During the studied period, 392 days were characterized by strong discharge values (higher than the mean multi-annual value of $300 \text{ m}^3.\text{s}^{-1}$ (Stoichev et al., 2004). In our MODIS database , 65 cloud-free images were available during the same period meaning that 17% of the over-average river flood events can be studied. All these images are available during decreasing discharge periods following flood peaks, when cloud-coverage decreases. Similar limitations nevertheless apply when using video camera monitoring systems or *in-situ* measurements, as stormy climatic conditions decrease the video images quality (Dailloux, 2008) and shipboard surveys and sampling data quality are highly dependent of the wind and sea conditions (Nezlin et al., 2007). It means that, whatever the monitoring system employed, it is difficult to describe the Adour River turbid plume during maximum flood events and that the maximum river plume extent or maximal mineral concentrations discharged through the Adour River turbid plume might be underestimated. Furthermore, strong wind conditions are underrepresented in our MODIS series (Fig. 3b).

Despite these climatic limitations, the MODIS database use in this study offer a synoptic and frequent overview of the Adour River turbid plume. The good representativeness of our satellite database (Figure 3) allowed describing its spatio-temporal variability and the spatial risk of exposure from turbid Adour waters to inshore marine waters for the first time over a multi-annual time period. Supervised methodology using a threshold value for delineating surface river plume

boundaries have been used in the literature and validated by previous studies (e.g. Devlin et al., 2012; Dzwonkowski and Yan, 2005; Horner-Devine et al., 2009; Molleri et al., 2010; Nezlin et al., 2008, Saldías et al., 2012). In this study we worked with MSM-calibrated map processed by a regional polynomial algorithm (equation 1; Petus et al., 2010) and a 3 mg.l^{-1} threshold value. The algorithm used was validated through satellite/in-situ match-up evaluation and comparisons with 1000-m MSM operational maps produced by IFREMER, except for suspended matter concentrations higher than 30 mg.l^{-1} (Petus et al., 2010). Despite the uncertainty on higher MSM concentration simulations, this algorithm specifically developed by Petus (2009) and Petus et al. (2010) for our study area was considered the most accurate to estimate the mineral suspended matters discharged through the Adour River turbid plume. Indeed, a threshold method does not require accurate retrieval of satellite WQ proxies above the defined threshold (here 3 mg.l^{-1}) as such waters would be classified as 'river plume' anyway (Schroeder et al., 2012).

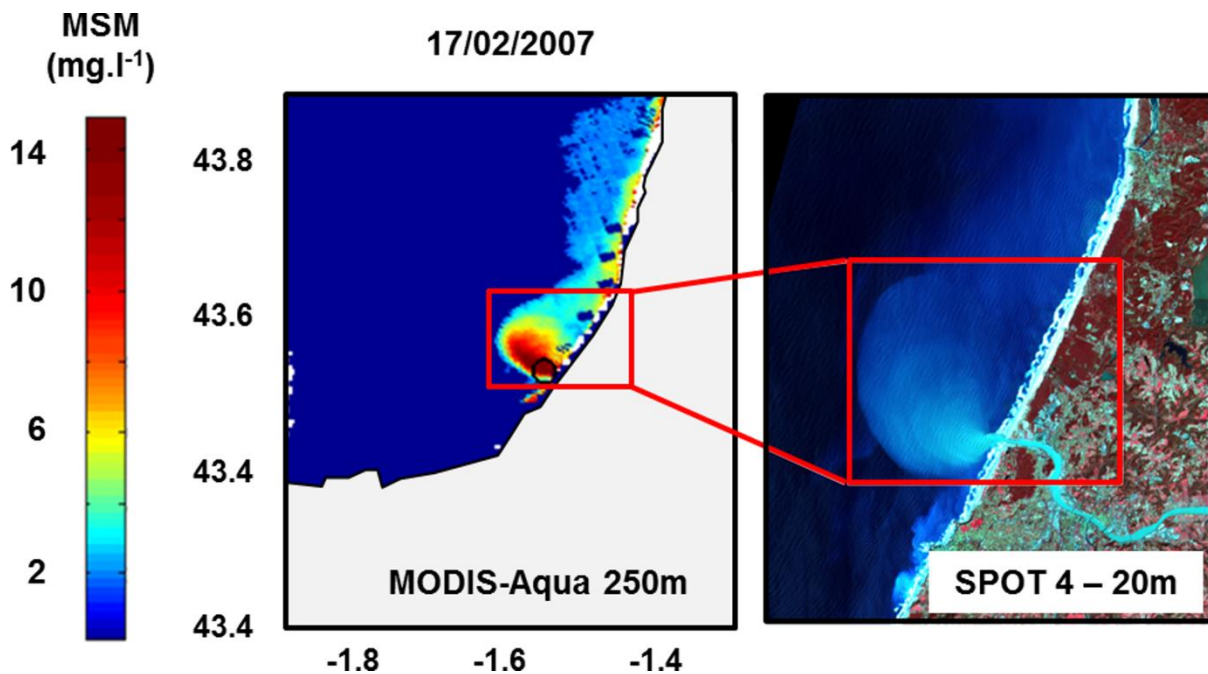


Figure 10: example of the Adour plume boundary estimated with the threshold methodology (left) and corresponding SPOT image (right, coloured compositions). The shape of the plume is well defined by the threshold methodology, although the high mineral suspended matters concentrations observed along the Landes coast may be associated to wave-generated resuspension of sediments.

The automated data analysis procedure was developed in order to eliminate most of the pixels contaminated by sediment resuspension or remaining clouds, and give the best estimation of the Adour River turbid plume surface boundaries. The Adour River turbid plume shape and orientation are well estimated even if sediment resuspension close to the coast may still affect some of the coastal pixels of the MSM maps used in this study (Figure 10). The differentiation of sediments discharged through the river and sediments resuspended by the action of the waves would require an analysis of their respective optical signatures (e.g. Novo et al., 1989), which is beyond the scope of this study. However, the image contamination via the resuspension processes is limited to the

coast and, over the time period considered, moderately impacts the Adour areas and MSM concentrations estimated from the satellite images as we do not observe bands of high risk of exposure from MSM > 3 mg.l⁻¹ along the coast on the multi-annual occurrence and mean maps (Figure 7). The 250-m resolution permits observing Adour River turbid plume shapes and also provide a detailed representation of the sediment gradients inside the river plume boundaries in comparison to 1-km satellite maps classically used to describe sediment behaviour in the studied area (Figure 11a and b).

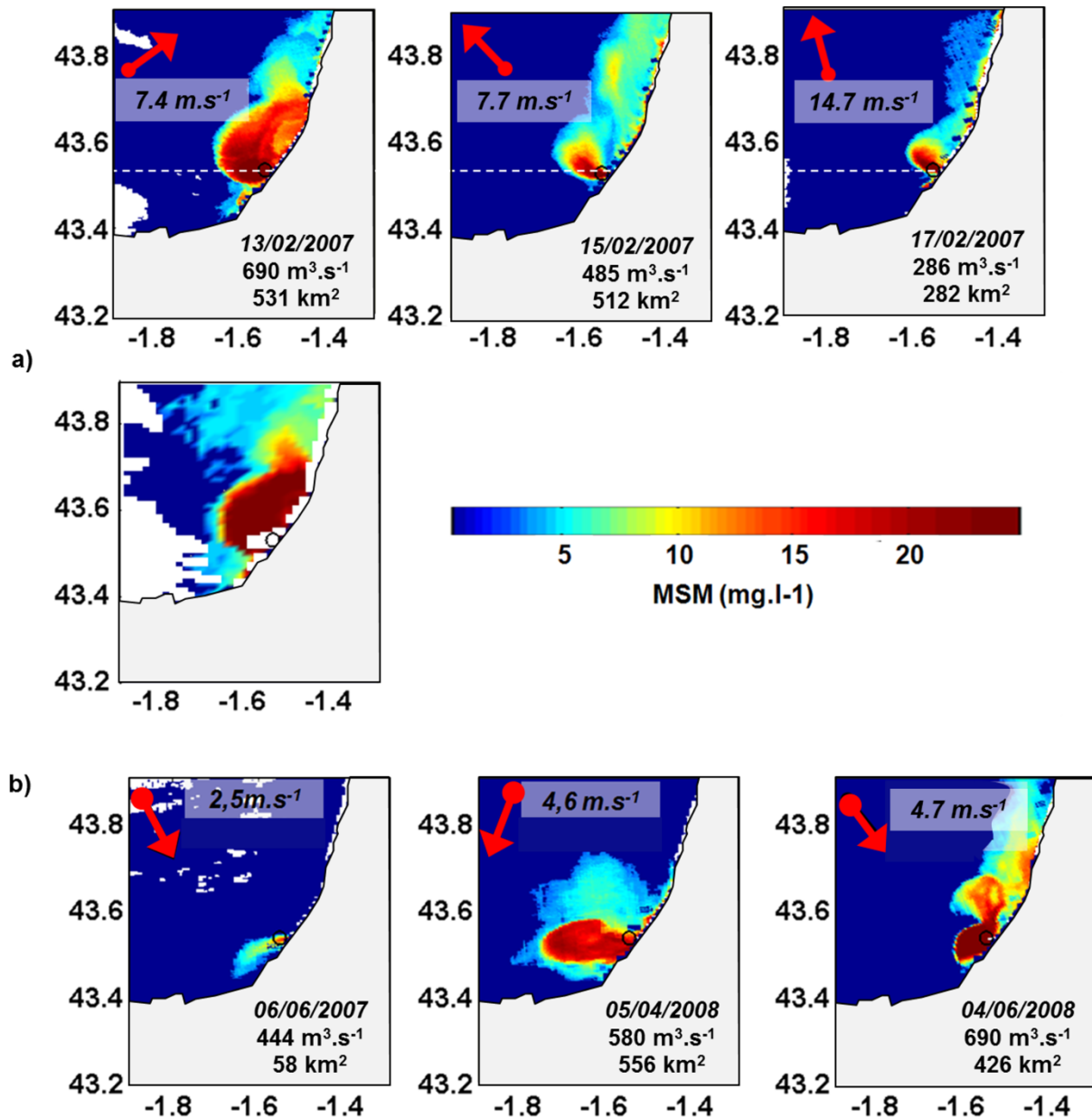


Figure 11: illustrations of the spatial variability affecting the Adour plume. a) Monitoring of the Adour lume during a falling period of river discharge and SE to SW winds. b) MODIS MSM 1-km map of the 13th of February 2007 calibrated with the Ifremer MSM algorithm (Image from the NAUSICAA website). c) Examples of plumes affected by northerlies winds. Days, outflows (m³.s⁻¹), wind speeds

(m.s-1) and plume areas (km²) are indicated in white. Wind orientations are symbolised by red arrows.

5.2. External controls on the spatio-temporal variability of the Adour River turbid plume

The Adour River turbid plume is an important oceanographic structure in the south-eastern Bay of Biscay (Figures 5 and 7). The multi-annual generated maps presented on Figure 7 form the basis of the first attempt at identifying the risk of exposure to coastal ecosystems from enhanced mineral suspended matters concentrations found in Adour River turbid plume waters and over a multi-annual time period. In our 2006-2009 satellite series, “plume-classified” pixels are observed 20% of the time up to 20 km north and 10 km south, and as far as 10 km offshore from the estuary mouth (Figure 7a). The spatial river plume influence is less extended within the southern coastal waters, although the frequency of river plume exposure is more important than in the north (river plume occurrence ~ 50% during the 2006-2009 period between the estuary mouth and the city of Biarritz). Based on forty-four 8-days 250-m resolution MODIS composites covering the year 2004, Sagarminaga et al. (2005) described the main area of influence of the Adour River turbid plume as a south-western oriented zone. Our results confirm this orientation when delineating the “main risk” area by an occurrence percentage higher than 50% (Figure 7a, orange to dark red colors). Under the influence of the Coriolis effect, the formation of anticyclonic bulges of circulating freshwater near the river mouth when the water exits the estuary has been widely described in the literature (e.g. Chao and Boitcourt, 1986; Chant et al., 2009) and observed in our study area by a local video camera system installed close to the Adour mouth (Dailloux, 2008; Morichon et al., 2008). Under light wind condition, Dailloux (2008) reported the development of this fresh and turbid bulge toward the west, north-west with its southern part impacting the southern beaches close to the estuary mouth. This phenomenon could be one explanation for the higher exposure level recorded on the south of the estuary (Figure 7).

The results of this study show that the Adour River turbid plume is a highly reactive system mainly controlled by the modulation of river discharge rates. Thus, the Adour discharge rates measured on same days that the satellite acquisitions explain 50 to 60 % of the river plume surface areas as well as MSM concentration indices (C_{max} and C_{mean}) variances (Figure 7a). The lower determination coefficients obtained when using 1 to 3 days lag between the discharges and the MSM data confirm that the sedimentation rates are low in the estuary and that most of sediment inputs from the river are rapidly exported to the ocean (Maneux et al., 1999). Using the linear regression computed between the Adour River discharge rates and river plume extends (Figure 8a), results show that river plume surface areas simulated from the Adour discharge rates are well correlated to the satellite-retrieved river plume surface areas (Figure 12). This further confirms the importance of river discharge rates on the control of the river plume surface area.

Wind conditions modulate the shape and orientation of the Adour River turbid plume, in agreement with theoretical models (Geyer et al., 2004; Wiseman and Garvine, 1995) and sporadic local observation/simulations of Dailloux (2008) and Jegou et al. (2001). Theoretical models describe that: (i) in the absence of strong external forcing, a northern hemisphere river plume turns to the right

forming an anticyclonic bulge of fresh water near the river mouth, attach to the coast, forming a buoyant coastal current flowing downstream in the direction of propagation of a kelvin wave; (ii) under downwelling-favorable winds (*i.e.*, blowing to the right looking offshore in the Northern Hemisphere) the coastal current velocity is increased and the river plume is narrowed and attached to the shore (Geyer et al., 2004) and, (iii), inversely, upwelling-favorable winds broaden and slow down the river plume expansion toward the North or reverse its direction (Geyer et al., 2004; Wiseman and Garvine, 1995). Our results confirm these circulation models. Indeed, under southern winds, we observed maximum Adour River turbid plume exposure toward the North and attached to the coast (Figure 9b) particularly when winds are S-SW orientated (figure 9b). This is also illustrated by a high-frequency satellite monitoring of the river plume during a falling period of river discharge with SE to SW winds (Figure 11a). High occurrences of MSM larger than 3 mg.l^{-1} observed along the northern coast (Figure 9b) are probably the signature of the development of a buoyant coastal current northward following the river plume attachment to the coast (Geyer et al., 2004; Wiseman and Garvine, 1995), even though the influence of sediments resuspended by waves cannot be totally rejected. Western winds also push the turbid freshwater toward the coast but is less supportive of the alongshore current development (Figure 9c).

Inversely, under Northern winds, the river plume exposure risk is reduced up North whereas maximum exposure is observed toward the South-West (Figure 9d). Furthermore, our database indicates that this plume reversion again the earth rotation effect is controlled by the wind intensity, but also by the river outflow velocity. As an example, a perfect south deviated river plume is observed on the 6th of June 2007 (Figure 11c) under relatively weak wind and medium discharge conditions (2.5 m.s^{-1} and $444 \text{ m}^3.\text{s}^{-1}$, respectively), whereas stronger winds measured on the 5th of April 5 and 4th of June 2007 ($> 4.6 \text{ m.s}^{-1}$) during stronger discharge periods ($> 580 \text{ m}^3.\text{s}^{-1}$) failed to completely deviate the river plume. Finally, we observe that eastern (NE to SE) winds promote the Adour River turbid plume advection on the continental shelf (Figure 9a). When the river discharges are high and the river plume well developed, this wind orientation increase the size of the Adour River turbid plume. As an illustration of this phenomenon, large river plume surface underestimated by the linear relationship between the Adour discharge rates and the river plume extent are systematically associated to eastern wind conditions (Figure 12).

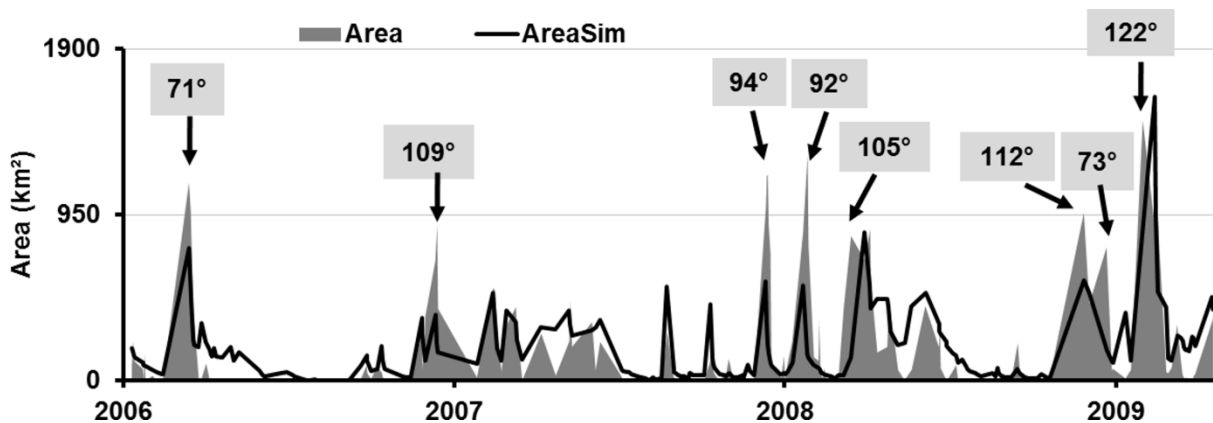


Figure 12: satellite-retrieved plume areas from our Modis database (grey surfaces) and simulated from the Adour river outflow values (black line) using the linear relationship computed on Figure 8a ($\text{Area} = 0.81 \cdot \text{River Outflow} - 56.59$). Wind origin directions ($^{\circ}$) for a selection of large plumes are indicated within grey rectangles. Large surface overestimated are systematically associated with Eastern winds

Eastward wind-driven currents promoting large freshwater transport toward the shelf break have also been recently described by Schiller et al. (2011) though numerical simulations of the Mississippi River plume (Gulf of Mexico). Timing of winds, floods and waves *i.e.*, the coherence of river and ocean conditions also influence coastal transport patterns and burial of sediment (Kniskern et al., 2011).

5.3 Seasonal climatology of the Adour River turbid plume

Despite the spatial and temporal limitations outlined in 5.1, the good representativeness of the MODIS database selected and the supervised methodology developed in this study allows us defining the seasonal climatology of the Adour River turbid plume (Figure 13).

During the winter period, river discharge rates are high and the Adour River turbid plume is spatially developed and concentrated in mineral suspended matters (Figure 8b and 13). Western regular winds (Figure 3) deviate the turbid freshwater towards the northern (Landes) coastline. During the spring season, river discharges start to decrease and winds are more variable (Figure 3). In response, the Adour River turbid plume is less expanded, less concentrated and mostly W-NW orientated (Figure 8b and 13). Hence, the Landes/northern coastal waters are less affected by the river plume during the spring season. During the drier summer period, the river plume influence in the south-eastern Bay of Biscay is highly reduced (Fig. 8b and 13). In October, the river plume starts to spread out again and the maximal geographic and sedimentary impact of the river plume during the autumn period is recorded in our series during the December month when both, northern and southern coastal waters, are affected by the river plume.

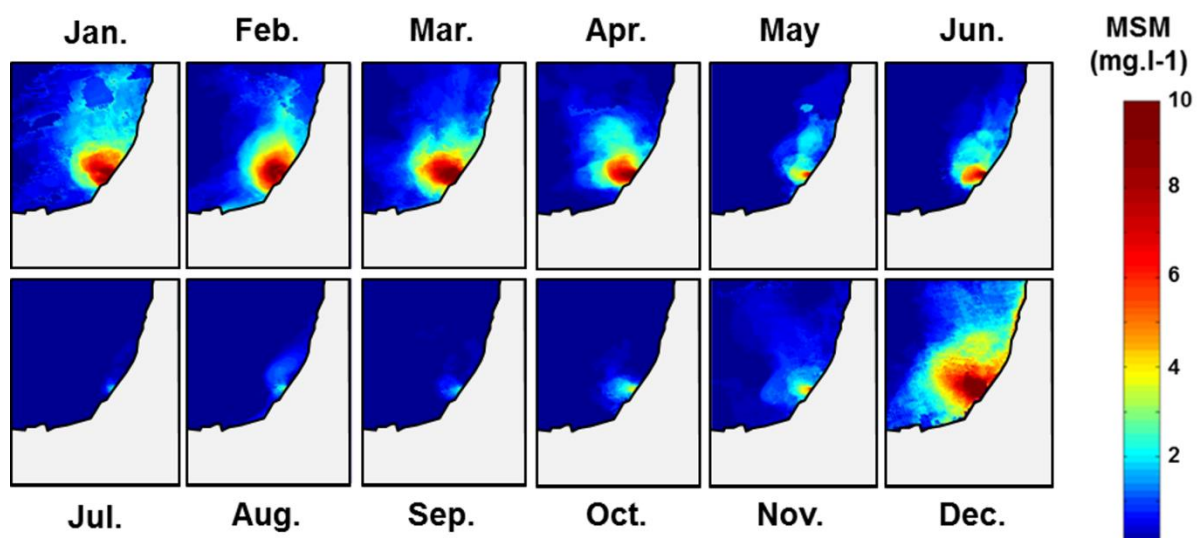


Figure 13: mean monthly MSM concentration maps calculated from the 246 MODIS images selected.

This regional model of evolution constitutes the first attempt to systematically map and study the seasonal Adour River turbid plume variability from satellite images at a relatively high-resolution, and over a multi-annual time-period. The results obtained extend the preliminary results obtained by Jegou et al. (2001). Using a 3D model, their one-year (1995) simulation described (i) low-salinity waters advected close to the coast northward or north-westward during February; (ii) river plumes spreading over the continental shelf in spring; and (iii) disappearance of the low-salinity Adour signature in summer. Our local results are furthermore in agreement with the recent study of Saldías et al., 2012 which describes the seasonal area cover of plume water off central Chile significantly correlated with seasonality in river discharge and modulated by wind orientations.

From a regional perspective, identifying the extent of riverine influence and areas most likely to be exposed to pollutants is particularly important during the summer period (June to September), when tourism is maximal and pollution of the coastal waters through contaminated river waters may have important sanitary repercussions. Our results demonstrate that, during the summer period, the Adour River turbid plume area is reduced and limited to an area close to the estuary mouth in response to low Adour River discharge rates (Figure 8b and 13). However, the mean Adour River turbid plume area and MSM concentrations (Area = 115 km², C_{max} = 16 mg.l⁻¹) observed during June are higher than in other summer months (Figure 8b and 13). During the summer season, river discharge rates are in average low, floods are rare, and therefore a large part of the sedimentary material is accumulated within the Adour watershed (Coynel et al., 2005). When the Adour discharge increases during episodically summer flood events, a significant quantity of this material is purged and directly discharged in the coastal waters in the form of a large turbid river plume. This is well illustrated by the extended and concentrated (over 20 mg.l⁻¹) river plume recorded the 6th of June 2008 (Figure 11b).

5.4 Future improvements of the method

Improvements of the automated method developed in this study are required to increase our knowledge of the impact of the Adour River turbid plume on the coastal water quality of the southern Bay of Biscay. First of all, increasing the number of satellite data (*i.e.*, include Terra data or expand MODIS-Aqua time series over a decadal scale) would potentially increase the number of ocean color data matching different wind and/or river flow conditions and increase the temporal representativeness of the satellite database. Higher resolution and more frequent images (hourly scale) would be necessary to better characterize smaller geographical and higher scale phenomena such as the influence of the tide on the spreading of river plume or the local scale (scale of local beaches for example) water quality impact of the Adour River turbid plume. Even if the river plume expansions and concentrations were shown higher during low tidal heights and high tidal coefficients (Table 1), the spatial (250-m) and temporal (1 image per day) resolution of the MODIS images prevented an accurate description of the tide influence on the spatio-temporal variability of the Adour River turbid plume. The higher observation frequency and spatial resolution offered by a camera monitoring system is more adapted to evaluate the effect of tides (Dailloux, 2008, Morichon, 2008); hence, a combination of remote sensing systems is suggested. Furthermore, it would be interesting to include the influence of coastal currents, wave energy, or bathymetry computed by

numerical modelling for producing a complete assessment of coastal areas exposed to the Adour River turbid plume.

Further validation of the empirical algorithm (equation 1) and atmospheric corrections used would also improve the monitoring effort undertaken in this study. Finally, scale the satellite-retrieved spatial and temporal information (*i.e.*, the risk of exposure to coastal ecosystems from Adour river waters) with relevant *in situ* water quality measurements such as nutrient (enhancing phytoplankton production), pollutant or bacterial (threatening ecosystem and human health) loads would be necessary to assess exposure of ecosystems to land-based pollutants discharged through the Adour River mouth. As demonstrated by this study, despite relatively small size of the Adour River, the Adour River turbid plume can have a non-negligible impact on the water quality of the southern bay of Biscay. The MSM and contaminants/nutrients transported within the Adour turbid river plume have the potential to be disseminated far away along the northern shoreline (southern winds), regularly over the southern boundaries of the Adour estuary (enhanced when winds are northerlies) and toward the shelf break (eastern winds). Methodologies combining remotely sensed and in-situ water quality data are, for example, developed for the protection of the Great Barrier Reef Ecosystems in Queensland, Australia (e.g. Devlin et al., 2012).

6. Conclusion

An automated MODIS-based tool was developed to map the mineral suspended matter discharged through the Adour River turbid plume within the south-eastern Bay of Biscay. We generate maps of the MSM concentration using a regional empirical algorithm and delineate the Adour turbid influence by a 3 mg.l⁻¹ MSM concentration threshold. Indices characterizing the physical and sedimentary variability of the Adour River turbid plume were systematically computed for a selection of 246 cloud-free days between January 2006 and April 2009. The Adour River turbid plume was shown to be an important oceanographic structure in the south-eastern Bay of Biscay and its behaviour mainly controlled by the variability of river discharge rates and wind orientation and strength. Main patterns of the river plume were described over multi-annual and seasonal scales. The risk of exposure to coastal ecosystems from the Adour River turbid plume waters were described for the first time based on temporally representative data. This first monitoring of the multi-annual Adour River turbid plume spatio-temporal variability proved the potential of 250-m MODIS images to support management and assessment of the water quality in the south-eastern Bay of Biscay. Although cloud coverage prevented to describe the river plume related to the stronger flood events, remote sensing imagery enhanced our knowledge of this turbid river plume. Collection of new data is necessary for a better validation of the regional algorithm used in this study. Complemented by geochemical (e.g. land based contaminants load rates) and biological information, use of MODIS imagery over several decades could become a powerful tool for monitoring potential impacts of the Adour River turbid plume on the ecological and sanitary health of the southern French coastal waters.

Acknowledgements

The authors would like to acknowledge the sponsors of this project: the Technical Littoral Center of the Lyonnaise des eaux of Biarritz, the Basque Water Agency (URA) and the Funds for Aquitania–Euskadi cooperation (Basque Government and Aquitaine Region).

Appendix A See Fig. A1.

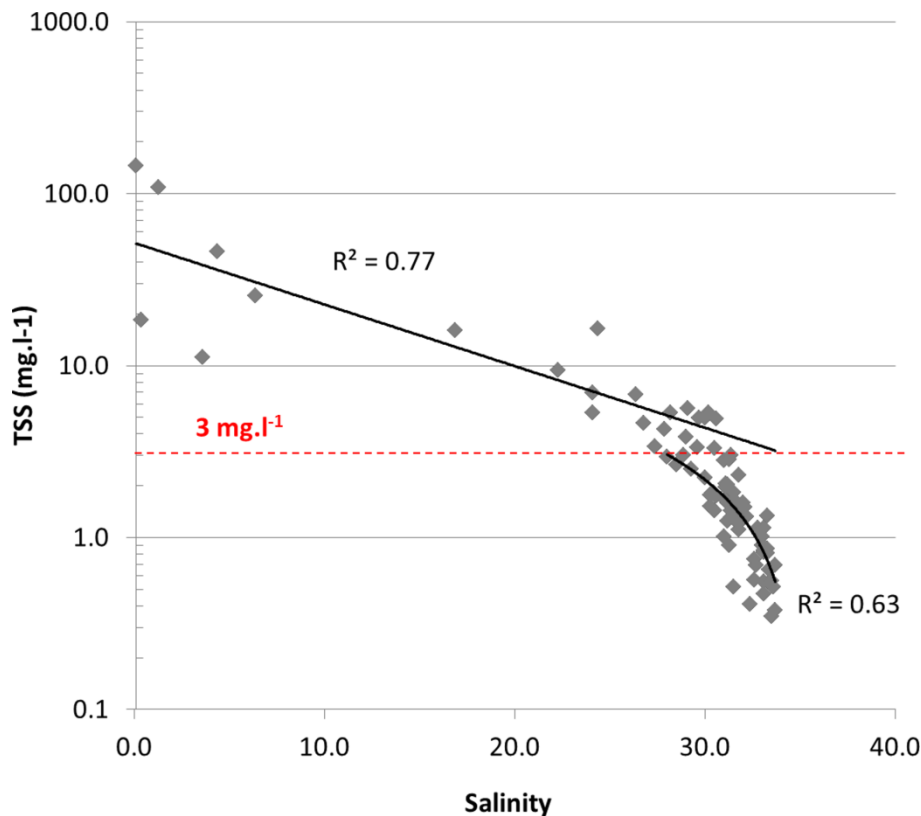


Fig. A1. (Appendix): relationship between the salinity and TSS measured in-situ during theBATEL-1survey. In-situmeasurementsduringtheBATEL-1surveyare described in Petus et al. (2010).

References

- Abadie, S., Butel, R., Dupuis, H., & Brière, C. (2005). Statistical parameters of waves on the south Aquitaine Coast. *Parametres statistiques de la houle au large de la côte sud-aquitaine*, 337, 769-776.
- Arleny, I., Tabouret, H., Rodriguez-Gonzalez, P., Bareille, G., Donard, O.F.X., & Amouroux, D. (2007). Methylmercury bioconcentration in muscle tissue of the European eel (*Anguilla anguilla*) from the Adour estuary (Bay of Biscay, France). *Marine Pollution Bulletin*, 54, 1031-1036.
- Artigas, L.F. (1998). Seasonal variability in microplanktonic biomasses in the Gironde dilution plume (Bay of Biscay): Relative importance of bacteria. *Oceanologica Acta*, 21, 563-580.

- Bareille, G., Amouroux, D., Donard, O., Lespes, G., Potin-Gautier, M., Caumette, P., Duran, R., Goni, M.S., Guyoneaud, R., Salvado, J.C., Budzinski, H., Garrigues, P., LeMenach, K., & Peluhet, L. (2006). Rivières pyrénéennes du piémont atlantique : de l'érosion des sols à la pollution chimique et microbienne. In, Cahier technique ECOBAG n°1/4 (p. 24).
- Baith, K., Lindsay, R., Fu, G., McClain, C.R. (2001). SeaDAS, a data analysis system for ocean colour satellite sensors. *Eos Trans. AGU*, 82: 202.
- Bergeron, P. (2007). Qualité microbiologique des eaux de baignade : des situations subies de pollution littorale à la gestion active des plages. Le cas d'Anglet et Biarritz. Published PhD thesis: Université Bordeaux 1.
- Borja, A., Galparsoro, I., Irigoien, X., Iriondo, A., Menchaca, I., Muxika, I., Pascual, M., Quincoces, I., Revilla, M., Germán Rodríguez, J., Santurtún, M., Solaun, O., Uriarte, A., Valencia, V., Zorita, I., 2011. Implementation of the European marine strategy framework directive: a methodological approach for the assessment of environmental status, from the Basque country (Bay of Biscay). *Marine Pollution Bulletin* 62, 889–904.
- Brodie, J., Schroede, T., Rohd, K., Faithful, J., Masters, B., Dekker, A., Brando, V., Maughan, M. (2010). Dispersal of suspended sediments and nutrients in the Great Barrier Reef lagoon during river-discharge events: conclusions from satellite remote sensing and concurrent flood-plume sampling. *Marine and Freshwater Research* 61(6), 651–664.
- Brunet, R.C., & Astin, K.B. (1999). Spatio-temporal variation in some physical and chemical parameters over a 25-year period in the catchment of the river Adour. *Journal of Hydrology*, 220, 209-221.
- CERSAT-IFREMER, 2002. Mean Wind Fields (MWF product) - User Manual - Volume 2: QuikSCAT.
- Chant, R.J., S.M. Glenn, E. Hunter, J. Kohut, R.F. Chen, R.W. Houghton, J. Bosch, and O. Schofield. (2009). Bulge Formation of a Buoyant River Outflow. *Journal of Geophysical Research*, 113(C1).
- Chao, S.Y., Boicourt, W.C. (1986). Onset of Estuarine Plumes. *Journal of Physical Oceanography*, 16, 2137–2149.
- Chen, Z., Hu, C., Muller-Karger, F. (2007). Monitoring turbidity in Tampa bay using MODIS/Aqua 250-m imagery. *Remote Sensing of Environment* 109 (2), 207–220.
- Coynel, A. (2005). Erosion mécanique des sols et transferts géochimiques dans le bassin Adour-Garonne. Published PhD Thesis. Bordeaux: University Bordeaux 1.
- Dailloux, D. (2008). Video measurements of the Adour plume dynamic and its surface water optical characteristics. Published PhD thesis: Université de Pau et des Pays de l'Adour.
- Dagg, M., Benner, R., Lohrenz, S., Lawrence, D. (2004). Transformation of dissolved and particulate materials on continental shelves influenced by large rivers: plume processes, *Continental Shelf Research* 24(7–8), 833-858.

- Devlin, M., Brodie, J. (2005). Terrestrial discharge into the Great Barrier Reef Lagoon: nutrient behaviour in coastal waters, *Marine Pollution Bulletin* 51, 9–22
- Devlin, M., Best, M., & Haynes, D. (2007). Implementation of the Water Framework Directive in European marine waters. *Marine Pollution Bulletin*, 55, 1-2.
- Devlin, M.J., McKinna, L.W., Alvarez-Romero, J.G., Petus, C., Abott, B., Harkness, P., Brodie, J., (2012). Mapping the pollutants in surface riverine flood plume waters in the Great Barrier Reef, Australia, 65(4–9), 2012, 224–235.
- Doxaran, D., Froidefond, J.M., Castaing, P., & Babin, M. (2009). Dynamics of the turbidity maximum zone in a macrotidal estuary (the Gironde, France): Observations from field and MODIS satellite data. *Estuarine, Coastal and Shelf Science*, 81, 321-332.
- Dwyer, J., & Schmidt, G. (2006). The MODIS reprojection tool. In J. J. Qu, W. Gao, M. Kafatos, R. E. Murphy & V. V. Salomonson (Eds.), *Earth science satellite remote sensing* Berlin Heidelberg: Springer Berlin Heidelberg.
- Dzwonkowski, B., & Yan, X.-H. (2005). Tracking of a Chesapeake Bay estuarine outflow plume with satellite-based ocean color data. *Continental Shelf Research*, 25, 1942-1958.
- Edmond, J.M. Boyle, E.A., B. Grant, Stallard, R.F. 1981. The chemical mass balance in the Amazon plume I: The nutrients. *Deep Sea Research Part A. Oceanographic Research Papers*, 28(11), 1339-1374.
- Etcheber, H., Taillez, A., Abril, G., Garnier, J., Servais, P., Moatar, F., & Commarieu, M.V. (2007). Particulate organic carbon in the estuarine turbidity maxima of the Gironde, Loire and Seine estuaries: Origin and lability. *Hydrobiologia*, 588, 245-259.
- Ferreira, J.G., Andersen, J.H., Borja, A., Bricker, S.B., Camp, J., 2011. Overview of eutrophication indicators to assess environmental status within the European Marine Strategy Framework Directive. *Estuarine, Coastal and Shelf Science* 93, 117–131.
- Ferrer, L., Fontáñin, A., Mader, J., Chust, G., González, M., Valencia, V., Uriarte, A., & Collins, M.B. (2009). Low-salinity plumes in the oceanic region of the Basque Country. *Continental Shelf Research*, 29, 970-984.
- Froidefond, J.M., Castaing, P., Mirmand, M., & Ruch, P. (1991). Analysis of the turbid plume of the Gironde (France) based on SPOT radiometric data. *Remote Sensing of Environment*, 36, 149-163.
- Froidefond, J.M., & Doxaran, D. (2004). Télédétection optique appliquée à l'étude des eaux côtières. *Télédétection*, 4, 579 – 597.
- Froidefond, J.M., Jegou, A.M., Hermida, J., Lazure, P., & Castaing, P. (1998). Variability of the Gironde turbid plume by remote sensing. Effects of climatic factors. *Oceanologica Acta*, 21, 191-207.
- Geyer, W.R., Hill, P.S., & Kineke, G.C. (2004). The transport, transformation and dispersal of sediment by buoyant coastal flows. *Continental Shelf Research*, 24, 927-949.

- Gohin, F., Druon, J.N., & Lampert, L. (2002). A five channel chlorophyll concentration algorithm applied to Sea WiFS data processed by SeaDAS in coastal waters. *International Journal of Remote Sensing*, 23, 1639-1661.
- Gohin, F., Loyer, S., Lunven, M., Labry, C., Froidefond, J.M., Delmas, D., Huret, M., & Herbland, A. (2005). Satellite-derived parameters for biological modelling in coastal waters: Illustration over the eastern continental shelf of the Bay of Biscay. *Remote Sensing of Environment*, 95, 29-46.
- Hewitt, J.H., & Mason, J. (1990). Synoptic inventory of riparian ecosystems: The utility of Landsat Thematic Mapper data. *Forest Ecology and Management*, 33-34, 605-620.
- Horner-Devine, A.R., Jay, D.A., Orton, P.M., & Spahn, E.Y. (2009). A conceptual model of the strongly tidal Columbia River plume. *Journal of Marine Systems*, 78, 460–475.
- Hu, C., Chen, Z., Clayton, T.D., Swarzenski, P., Brock, J.C., Muller-Karger, F. (2004). Assessment of estuarine water-quality indicators using MODIS medium-resolution bands: initial results from Tampa Bay, FL. *Remote Sensing of Environment* 93 (3), 423–441.
- Jegou, A.M., Dumas, F., & Lazure, P. (2001). Modelling the Adour plume with a 3D hydrodynamic model. In, *Colloque international d'océanographie du Golfe de Gascogne N°7* (pp. 49 - 54). Biarritz.
- Jeng, H.A.C., Engle, A.J., Baker, R.M., & Bradford, H.B. (2005). Impact of urban stormwater runoff on estuarine environmental quality. *Estuarine, Coastal and Shelf Science*, 63, 513-526.
- Kaufman, Y.J., Tanre', D., Remer, L.A., Vermote, E.F., Chu, A., Holben, B.N. (1997). Operational remote sensing of tropospheric aerosol over land from EOS moderate resolution imaging spectroradiometer. *Journal of Geophysical Research* 102, 17051–17067.
- Kniskern, T.A., J.A. Warrick, K.L. Farnsworth, R.A. Wheatcroft, M.A. Goñi. (2011). Coherence of river and ocean conditions along the US West Coast during storms. *Continental Shelf Research*, 31, 789-805.
- Labry, C., Delmas, D., & Herbland, A. (2005). Phytoplankton and bacterial alkaline phosphatase activities in relation to phosphate and DOP availability within the Gironde plume waters (Bay of Biscay). *Journal of Experimental Marine Biology and Ecology*, 318, 213-225.
- Lahet, F., Stramski, D. (2010). MODIS imagery of turbid plumes in San Diego coastal waters during rainstorm events. *Remote Sensing of Environment* 114, 332–344.
- Lazure, P., & Jegou, A.M. (1998). 3D modelling of seasonal evolution of Loire and Gironde plumes on Biscay Bay continental shelf. *Oceanologica Acta*, 21, 165-177.
- Lee, J., Valle-Levinson, A. (2013). Bathymetric effects on estuarine plume dynamics. *Journal of Geophysical Research C: Oceans*, 118(4), 1969-1981
- Lentz, S. J., and J. Largier. (2006). The Influence of Wind Forcing on the Chesapeake Bay Buoyant Coastal Current. *Journal of Physical Oceanography*, 36, 1305-1316.

- Lihan, T., Saitoh, S.-I., Iida, T., Hirawake, T., & Iida, K. (2008). Satellite-measured temporal and spatial variability of the Tokachi River plume. *Estuarine, Coastal and Shelf Science*, 78, 237-249.
- Maneux, E. (1998). Erosion mécanique des sols et transports fluviaux de matières en suspension : Application des systèmes d'information géographique dans les bassins versants de l'Adour, de la Dordogne et de la Garonne. In (p. 252): Bordeaux 1.
- Maneux, E., Dumas, J., Clement, O., Etcheber, H., Charritton, X., Etchart, J., Veyssy, E., & Rimmelin, P. (1999). Assessment of suspended matter input into the oceans by small mountainous coastal rivers: The case of the Bay of Biscay. *Comptes Rendus de l'Academie de Sciences - Serie IIa: Sciences de la Terre et des Planetes*, 329, 413-420.
- Miller, R.L., McKee, B.A. (2004). Using MODIS Terra 250 m imagery to map concentrations of total suspended matter in coastal waters. *Remote Sensing of Environment* 93 (1–2), 259–266.
- Moller, G.S.F., de M. Novo, E.M.L., & Kampel, M. (2010). Space-time variability of the Amazon River plume based on satellite ocean color. *Continental Shelf Research*, 30, 342-352.
- Monperrus, M., Point, D., Grall, J., Chauvaud, L., Amouroux, D., Bareille, G., & Donard, O. (2005). Determination of metal and organometal trophic bioaccumulation in the benthic macrofauna of the Adour estuary coastal zone (SW France, Bay of Biscay). *Journal of Environmental Monitoring*, 7, 693-700.
- Morichon, D., Dailloux, D., Aarninkhof, S., & Abadie, S. (2008). Using a shore-based video system to hourly monitor storm water plumes (Adour River, Bay of Biscay). *Journal of Coastal Research*, 24, 133-140.
- Nezlin, N.P., DiGiacomo, P.M., Diehl, D.W., Jones, B.H., Johnson, S.C., Mengel, M.J., Reifel, K.M., Warrick, J.A., & Wang, M. (2008). Stormwater plume detection by MODIS imagery in the southern California coastal ocean. *Estuarine, Coastal and Shelf Science*, 80, 141-152.
- Nezlin, N.P., DiGiacomo, P.M., Jones, B.H., Reifel, K.M., Warrick, J.A., Johnson, S.C., & Mengel, M.J. (2007). MODIS imagery as a tool for synoptic water quality assessments in the southern California coastal ocean. In, *Proceedings of SPIE - The International Society for Optical Engineering*.
- Novo, E. M. M. Hansom, J. D., Curran, P. J. 1989. The effect of sediment type on the relationship between reflectance and suspended sediment concentration *International Journal of Remote Sensing*, 10(7), 1283-1289.
- Novoa, S., Chust, G., Froidefond, J.M., Petus, C., Franco, J. Orive, E. Seoane, S. Borja, A. (2012a). Water quality monitoring in Basque coastal areas using local chlorophyll-a algorithm and MERIS images. *Journal of Applied Remote Sensing*, 6, 063519-1-27.
- Novoa, S., Chust, G., Sagarminaga, Y., Revilla, M., Borja, A. & Franco, J. (2012b) Water quality assessment using satellite-derived chlorophyll-a within the European directives, in the southeastern Bay of Biscay. *Marine Pollution Bulletin*, 64, 739-750.

- Novoa, S., Chust, G., Sagarminaga, Y., Revilla, M., Franco, J., Valencia, V., Borja, Á., (2012c). Chlorophyll-a variability within Basque coastal waters and the Bay of Biscay, between 2005 and 2010, using MODIS imagery. *Revista de Investigación Marina, AZTI-Tecnalia*, 19(5): 92-107
- Ondrusek, M., Stengel, E., Kinkade, C., Vogel, R., Keegstra, P., Hunter, C., Kim, C., 2012. The development of a new optical total suspended matter algorithm for the Chesapeake Bay. *Remote Sens. Environ.* 119, 243–254.
- Orton, P.M., and D.A. Jay. (2005). Observations at the tidal plume front of a high-volume river outflow. *Geophysical Research Letters*, 32(11).
- Petus, C. (2009). *Qualité des eaux cotières du sud du Golfe de Gascogne par télédétection. Méthodologie de détermination et de quantification de substances particulaires et dissoutes.* Published PhD Thesis. Bordeaux: University Bordeaux 1.
- Petus, C., Chust, G., Gohin, F., Doxaran, D., Froidefond, J.-M., & Sagarminaga, Y. (2010). Estimating turbidity and total suspended matter in the Adour River plume (South Bay of Biscay) using MODIS 250-m imagery. *Continental Shelf Research*, 30, 379-392.
- Point, D., Bareille, G., Amouroux, D., Etcheber, H., & Donard, O.F.X. (2007). Reactivity, interactions and transport of trace elements, organic carbon and particulate material in a mountain range river system (Adour River, France). *Journal of Environmental Monitoring*, 9, 157-167.
- Sagarminaga, Y., Chust, G., & Dailloux, D. (2005). Detección y seguimiento de la pluma del río Adour mediante MODIS. In *XI Congreso Nacional de Teledetección* (p. 4). Tenerife.
- Saldías, G.S., Sobarzo, M., Largier, J., Moffat, C., Letelier, R. (2012). Seasonal variability of turbid river plumes off central Chile based on high-resolution MODIS imagery. *Remote Sensing of Environment*, 123, 220–233.
- Schiller, R. V., Kourafalou, V. H., Hogan, P., Walker, N. D. (2011). The dynamics of the Mississippi River plume: Impact of topography, wind and offshore forcing on the fate of plume waters. *Journal of Geophysical Research*, 116, C06029, doi:10.1029/2010JC006883.
- Schroeder T, Devlin MJ, Brando VE, Dekker AG, Brodie JE, Clementson LA, McKinnon L. (2012). Inter-annual variability of wet season freshwater plume extent into the Great Barrier Reef lagoon based on satellite coastal ocean colour observations. *Marine Pollution Bulletin*, 65(4-9), 210-23.
- Stoichev, T., Amouroux, D., Wasserman, J.C., Point, D., De Diego, A., Bareille, G., & Donard, O.F.X. (2004). Dynamics of mercury species in surface sediments of a macrotidal estuarine-coastal system (Adour River, Bay of Biscay). *Estuarine, Coastal and Shelf Science*, 59, 511-521.
- Tabouret, H., Bareille, G., Mestrot, A., Caill-Milly, N., Budzinski, H., Peluhet, L., Prouzet, P., & Donard, O.F.X. (2011). Heavy metals and organochlorinated compounds in the European eel (*Anguilla anguilla*) from the Adour estuary and associated wetlands (France) *Journal of Environmental Monitoring*, 13, 1446-1456.
- Thomas, A.C., & Weatherbee, R.A. (2006). Satellite-measured temporal variability of the Columbia River plume. *Remote Sensing of Environment*, 100, 167-178.

Valente, A.S., and J.C.B da Silva. (2009). On the observability of the fortnightly cycle of the Tagus estuary turbid plume using MODIS ocean colour images. *Journal of Marine Systems*, 75, 131-137.

Vermote, E.F., El Saleoql, N., Justice, C.O., Kaufman, Y.J., Privette, J.L., Remer, L., Roger, J.C., Tanre', D. (1997). Atmospheric correction of visible to middle-infrared EOS-MODIS data over land surfaces: background, operational algorithm and validation. *Journal of Geophysical Research*, 102, 17131–17141.

Villate, F., Franco, J., Ruiz, A., & Orive, E. (1989). Caracterización geomorfológica e hidrológica de cinco sistemas estuáricos del País Vasco (1). *Kobie*, 18, 157–170.

Warrick, J.A., DiGiacomo, P.M., Weisberg, S.B., Nezlin, N.P., Mengel, M., Jones, B.H., Ohlmann, J.C., Washburn, L., Terrill, E.J., & Farnsworth, K.L. (2007). River plume patterns and dynamics within the Southern California Bight. *Continental Shelf Research*, 27, 2427-2448.

Wiseman Jr, W.J., & Garvine, R.W. (1995). Plumes and Coastal Currents Near Large River Mouths. *Estuaries and Coasts*, 18, 509 – 517.